Deep-Sea Research I 57 (2010) 125–142

Contents lists available at ScienceDirect

Deep-Sea Research I

journal homepage: www.elsevier.com/locate/dsri

Three-year assessment of particulate organic carbon fluxes in Amundsen Gulf (Beaufort Sea): Satellite observations and sediment trap measurements

Alexandre Forest [a,*], Simon Bélanger [b], Makoto Sampei [a], Hiroshi Sasaki [c], Catherine Lalande [a], Louis Fortier [a]

[a] Québec-Océan, Département de Biologie, Université Laval, Québec, Canada G1V 0A6
[b] Département de Biologie, Chimie et Géographie, Université du Québec à Rimouski, 300 allée des Ursulines, Rimouski, Canada G5L 3A1
[c] Senshu University of Ishinomaki, Ishinomaki, Miyagi 986-8580, Japan

ARTICLE INFO

Article history:
Received 21 January 2009
Received in revised form
22 September 2009
Accepted 2 October 2009
Available online 12 October 2009

Keywords:
Particulate organic carbon fluxes
Sequential sediment traps
Remote sensing
Environmental forcing
Inter-annual variability
Arctic Ocean

ABSTRACT

Surface concentrations and vertical fluxes of particulate organic carbon (POC) were assessed in the Amundsen Gulf (southeastern Beaufort Sea, Arctic Ocean) over the years 2004 to 2006 by using ocean color remote-sensing imagery and sequential sediment traps moored over the ca. 400 m isobath. Environmental conditions (sea ice, wind) and oceanographic variables (temperature, salinity, fluorescence and currents) were investigated to explain the variability of POC data. Annual downward POC fluxes in 2004, 2005 and 2006 cumulated, respectively, to 3.3, 4.2 and 6.0 g C m^{-2} yr^{-1} at ~100 m depth, and to 1.3, 2.2 and 3.3 g C m^{-2} yr^{-1} at ~210 m depth. The fraction of settling POC attributable to autochthonous processes occurring at or next to ice break-up was estimated to be 75–84% of the 100 m annual fluxes and to be 61–75% of the 210 m fluxes. Over the three ice-reduced seasons, distinct scenarios between ice conditions, surface POC pools and vertical POC export at 100 m were identified: (1) in 2004, despite a normal ice break-up, a weak primary production was measured and low vertical fluxes were collected as old ice moved across the region; (2) in 2005, a lengthened ice-free period allowed an extended season of surface POC production near-shore, while an intermediate increase of vertical fluxes was recorded offshore; and (3) in 2006, a late ice melt gave rise to a pulsed ice edge bloom and to large vertical fluxes also associated with extra ice-flushed material. Linear regressions of vertical POC fluxes against satellite-derived surface POC concentrations suggested that the pelagic POC retention in the upper 100 m of the Amundsen Gulf ranged from ca. 70% to 90% depending on the timing of ice cover melt. Regardless of the inter-annual variability, the estimated fraction of the surface POC reservoir reaching the 210 m water depth was reduced to ~5%. Therefore, as the Arctic Ocean warms up, our results support the expectation that the increasing extent of the seasonal ice zone will promote the POC pathways that benefit pelagic webs rather than benthic communities.

© 2009 Elsevier Ltd. All rights reserved.

1. Introduction

Fluxes of particulate organic carbon (POC) from the surface ocean to the deep sea are central processes in the regulation of atmospheric CO_2 and climatic changes, as well as key determinants in the distribution and abundance of benthic communities (e.g., Boyd and Trull, 2007; Buesseler et al., 2007; Honjo et al., 2008).

In the Arctic Ocean, the magnitude and nature of vertical POC fluxes are at first order linked to the forcing and the habitats created by sea ice conditions (e.g., Ramseier et al., 1999). First, the primary production rate by phytoplankton (mainly diatoms) is dictated by the variability of the ice/snow cover because it attenuates incident solar irradiance, reduces wind-driven mixing of deep nutrients and modulates thermal and haline stratification of the upper water column (Sakshaug, 2004; Carmack et al., 2006; Tremblay et al., 2008). These factors control the spring bloom dynamics, which largely determines how much new POC will be available for export on an annual basis (e.g., Wassmann et al., 2004; Tremblay et al., 2006). Second, the bottom part of the ice cover serves as a growth matrix for ice algae that secrete abundant quantities of viscous exopolymeric substances (Meiners et al., 2003). The release of this ice-retained biomass during the vernal ice melt supplies a rapid export of POC to depth (e.g., Riedel et al., 2006; Renaud et al., 2007; Forest et al., 2007). Third, it is suspected that the sea ice regime controls the match or mismatch between zooplankton grazers and primary production (Loeng et al., 2005). An early ice break-up in spring seems to shift POC pathways toward fuelling the pelagic food web instead of contributing to sinking downward fluxes to the

* Corresponding author. Present address: Norwegian College of Fishery Science, Department of Aquatic Biosciences, University of Tromsø, N-9037 Tromsø, Norway. Tel.: +47 77 64 55 65; fax: +47 77 64 60 20.
E-mail addresses: alexandre.forest@uit.no, alforest@videotron.ca (A. Forest).

0967-0637/$ - see front matter © 2009 Elsevier Ltd. All rights reserved.
doi:10.1016/j.dsr.2009.10.002

benthos (e.g., Bluhm and Gradinger, 2008). And fourth, by resuspending and advecting shelf particles offshore, thermohaline convection and eddy generation induced by sea ice formation are important engines for the shelf-basin transfer of POC (Backhaus et al., 1997; Forest et al., 2007; Mucci et al., 2008). The lateral supply of organic matter from the surrounding margins to the deep Arctic basin appears to be an efficient mechanism by which POC may be sequestered for thousands of years (Hwang et al., 2008).

The current trend in the lengthening of the open water season and the imminence of a seasonally ice-free ocean in the Arctic (Wang and Overland, 2009) thus raise questions on the future behavior of vertical POC fluxes (e.g., Forest et al., 2008a). Recent works suggest that the Arctic Ocean carbon sink has tripled from 1972 to 2002 mainly due to the sea ice cover removal that maintained surface waters under-saturated with respect to CO_2 (Bates et al., 2006), and that annual primary production has increased by ~25% from 1998 to 2007 (Pabi et al., 2008; Arrigo et al., 2008). In the meantime, the inter-annual variability of coupling between surface carbon pools and vertical POC export in Arctic waters remains poorly quantified (e.g., Michel et al., 2006; Lepore et al., 2007; Reigstad et al., 2008). Hence, forecasting the impact of sea ice retreat on core ecosystem variables, such as the timing, intensity and composition of downward POC fluxes, is still open to debate (e.g., Tremblay et al., 2006; Wassmann et al., 2006; Lalande et al., 2007). In this study, we hypothesize that POC export below the euphotic layer would be largest during a year of protracted ice-free conditions, leading to a more efficient biological pumping of CO_2 to depth.

Here we report on the seasonal and inter-annual variability (October 2003–September 2006) of vertical POC fluxes recorded at ~100 and ~210 m depth in the western Amundsen Gulf located in the southeastern Beaufort Sea (ca. 400 m isobath; Fig. 1). A compelling aspect of our study was to combine a 3-year dataset of moored sediment trap measurements with remote-sensing observations to document the relationships between vertical POC fluxes and surface POC concentrations during the open water period (i.e., ~June–September). Many investigations have already attempted to link surface ocean color and vertical particle fluxes (mainly at depths >1000 m) in diverse oceanic regimes (see Nodder et al., 2005). But despite the remarkable usefulness of satellite tools to understand marine systems, such a comparison has not yet been performed in the Arctic seas (cf. Pabi et al., 2008; Arrigo et al., 2008). Physical forcing parameters (sea ice, winds, surface/near-surface temperatures, currents) and water column profiles (temperature, salinity, fluorescence) are also presented to better interpret the POC data. The main objective was, therefore, to evaluate the influence of the environmental variables on the timing and magnitude of surface POC reservoirs and vertical POC fluxes within the epipelagic zone of the Amundsen Gulf region in the Arctic Ocean.

1.1. Study area

1.1.1. Geography and hydrography

The Amundsen Gulf is a large channel (~400 km length × 170 km width) that connects the southeastern Beaufort Sea to the Canadian Archipelago (Fig. 1). The mouth of the Gulf is bordered by the Banks Island Shelf (40 km × 250 km) to the north and by the Mackenzie Shelf (120 km × 530 km) to the southwest. The latter is strongly influenced by the Mackenzie River, which is fourth in terms of water discharge (~330 $km^3 yr^{-1}$), but first for particulate matter output (~124 $Tg yr^{-1}$) amongst Arctic rivers (Rachold et al., 2004). Since most of the Mackenzie River sediments (~97%) are deposited in the delta or near-shore (O'Brien et al., 2006), only a small amount of plume material can reach the Amundsen Gulf.

Simplified water masses in the Amundsen Gulf comprise the Polar-Mixed Layer (salinity of ~26–31, 0–50 m) that sits over the Pacific Halocline (~32–33, 50–200 m), which itself overlays

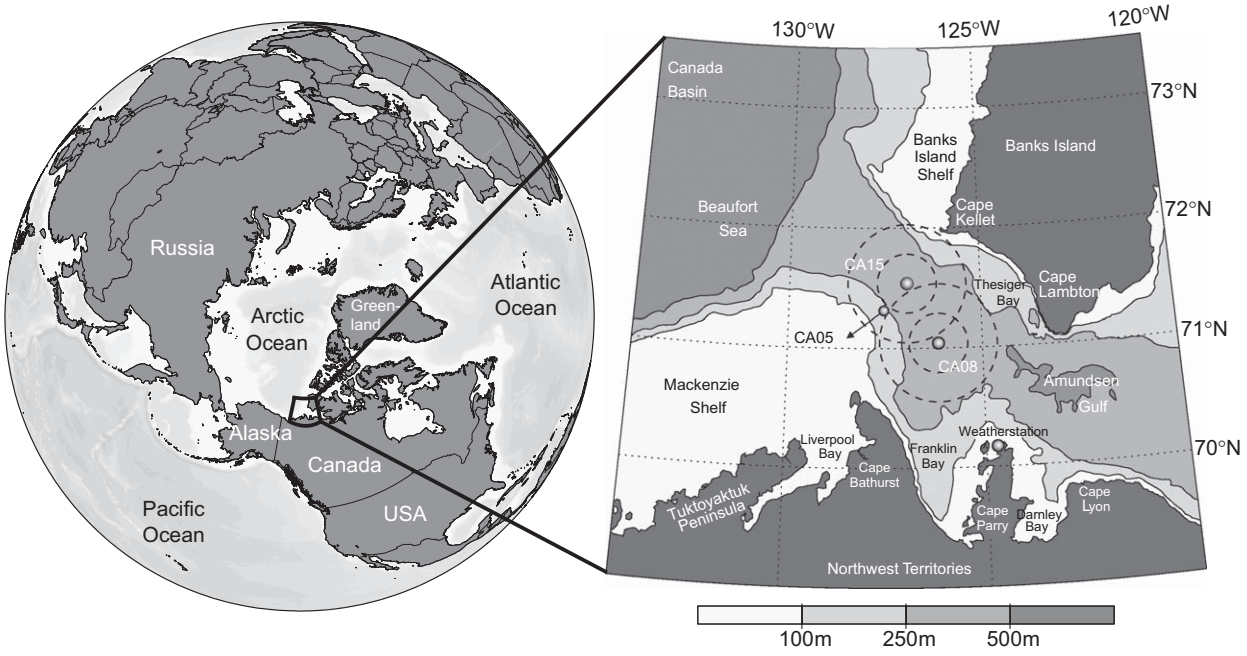

Fig. 1. Left map: Orthographic polar projection of the Northern Hemisphere showing the Mediterranean Arctic Ocean as a node between the Pacific and Atlantic oceans. Right map: Bathymetry of southeastern Beaufort Sea with the position of the two moorings equipped with sediment traps, T (°C)-probes and current meters (CA15 and CA08, both on the ca. 400 m isobath) in the western Amundsen Gulf. The CA15 and CA08 mooring points possess a 5 km radius, while the concentric circles over these moorings correspond to the 25 and 50 km radius areas. Surface POC concentrations were extracted from composite satellite images (Fig. 4) within each of the three circle areas. Also located on the right map: the DEW Line weather station at Cape Parry, where the winds were recorded; and the mooring CA05 (211 m isobath), where a T (°C)-probe was deployed in 2005–2006. The complete detail of mooring deployments is given in Table 1.

Atlantic Waters (≥ 34, >200 m) (Carmack and MacDonald, 2002). Surface circulation in the region is influenced by the westward branch of the anticyclonic Beaufort Gyre, but increasingly frequent reversals of this gyre have been observed in the last 30 years (Lukovich and Barber, 2006). In general, the surface flow at the mouth of the Amundsen Gulf is directed basinward, but depending on sea ice and wind conditions, surface waters may veer to the east toward the Canadian Archipelago (Ingram et al., 2008). Below 50 m depth, the Beaufort Undercurrent carries waters of both Pacific and Atlantic origin and flows eastward along the slope of the Beaufort Sea and into the Amundsen Gulf (Carmack and MacDonald, 2002; Ingram et al., 2008).

1.1.2. Sea ice, wind and primary production

Seasonal ice formation begins in October near the coasts and by late December the ice cover is consolidated over the region (Galley et al., 2008). In early April, a landfast ice bridge usually forms ($\sim$60% of the time over 1980–2007) directly south of Banks Island up to the continent (CIS, 2007). In these years, the sea ice retreat has typically begun in early June with the widening of the flaw lead network between Thesiger Bay and Franklin Bay (i.e., the Cape Bathurst Polynya), while in other years the ice break-up started with a shore lead extending eastward from Cape Parry (Galley et al., 2008). Westward surface stress induced by ice motion or winds triggers intermittent coastal upwelling near Cape Bathurst (Ingram et al., 2008). Easterly winds are dominant in spring and early summer, while westerly winds $>35\,km\,h^{-1}$ become more frequent from July to October (Ayles and Snow, 2002). Strong winds from the west–northwest are often responsible for intrusion of multi-year pack ice over coastal waters (e.g., Forest et al., 2008a).

From 1998 to 2004, primary production in the Amundsen Gulf has been estimated with different approaches. Between 1998 and 2002, remote sensing (SeaWiFS) indicated that annual total primary production rates varied from 90 to $175\,g\,C\,m^{-2}\,yr^{-1}$ in response to wind and sea ice dynamics (Arrigo and van Dijken, 2004). In the fall of 2002 and 2003, Brugel et al. (2009) used the ^{14}C-uptake method to estimate that total primary production cumulated to $\sim 3\,g\,C\,m^{-2}$ from mid-September to October. And from May to August 2004, *in situ* nutrient inventories in the Franklin Bay yielded a new primary production value of only $18\,g\,C\,m^{-2}$ (Tremblay et al., 2008).

2. Materials and methods

2.1. Sea ice, sea surface temperature and wind

Time-series of weekly averaged ice concentrations, expressed as a percent of the total sea area, and various stages of development (old, first-year, and new/young sea ice) from October 2003 to December 2006 in the western Amundsen Gulf (Fig. 1) were obtained with the Ice Graph Tool of the Canadian Ice Service (CIS; http://ice-glaces.ec.gc.ca/IceGraph/) using the specific region 'Amundsen Gulf Mouth' [cwa05_03]. IceGraph dataset is based on the collection of Regional Charts in the Geographic Information System of the CIS Digital Archive.

Available sea surface temperatures (SST) for the same region were extracted from the PO.DAAC Ocean ESIP Tool (http://poet.jpl.nasa.gov/) using the Moderate Resolution Imaging Spectroradiometer (MODIS-Aqua) level 3 SST product (nighttime, far-IR, best quality, spatial and temporal resolutions of 4.63 km and 1 day, respectively).

Hourly wind speeds and directions at the DEW Line weather station at Cape Parry (70°10.2′N, 124°43.2′W; Fig. 1) were obtained from the Weather Archive of Environment Canada (http://www.climate.weatheroffice.ec.gc.ca/). Monthly wind roses for the period of May–September in 2004, 2005 and 2006 were produced using the WindRose software (http://www.enviroware.com/).

2.2. Composite images of surface POC concentrations

More than 200 satellite images (free or partly-free of clouds) of the Amundsen Gulf region collected with the MODIS-Aqua sensor over the period of late May–September in 2004, 2005 and 2006 were acquired from the NASA Goddard Earth Sciences Data and Information Services Center (http://oceancolor.gsfc.nasa.gov) (Table 2). The Local Area Coverage (LAC, 1 km resolution) images at level 1A (top-of-atmosphere radiances) were processed to level 2 using the software SeaDAS (version 5.0.5). A regional POC algorithm developed and validated during the Canadian Arctic Shelf Exchange Study (CASES) in 2003–2004 was applied to L2 images using Interactive Data Language. For a complete methodology and discussion on the regional POC algorithm, see the Appendix.

Semi-monthly composites of surface POC concentrations (7 per year from late May to September) were generated using SeaDAS l3bin program. Pixels were excluded if any of the following L2 flags were set: sun zenith $>70°$, satellite sensor zenith $>60°$, cloud or ice, stray light, high sun glint, high top-of-atmosphere radiance, low water-leaving radiance at 555 nm (a flag used to identify cloud-shadowed pixels), or atmospheric correction failure and warning (Franz, 2005). An additional flag was used to eliminate pixels contaminated by the adjacency effect close to sea ice (Bélanger et al., 2007).

Mean surface POC concentrations of valid pixels were calculated within circle areas of 5, 25 and 50 km radius centered on the CA15 and CA08 moorings (Fig. 1, Table 1). These averages were extracted from each composite satellite image using a subset extraction routine implemented into the Generic Mapping Tools software package (http://gmt.soest.hawaii.edu/). The radii were chosen based on the two following assumptions: (1) vertical POC fluxes during the ice-reduced periods are primarily composed of

Table 1
Locations, periods of deployment and instrumentation detail of the moorings used in the present study.

Mooring	Date deployed	Latitude	Longitude	~35 m T (°C) sensor	~90 m current meter	~100 m sediment trap	~200 m current meter	~210 m sediment trap	Bottom depth (m)	Date recovered
CA15 (1st year)	10- Oct- 2003	71° 32.23′ N	127° 01.43′ W	ALEC (31 m)	ADCP (95 m)	Technicap (105 m)	RCM11 (200 m)	Nichiyu (210 m)	399	22- Jul- 2004
CA15 (2nd year)	24- Jul- 2004	71° 32.26′ N	127° 01.45′ W	ALEC (33 m)	ADCP (97 m)	Technicap (107 m)	RCM11 (202 m)	Nichiyu (212 m)	398	3- Sep- 2005
CA08 (3rd year)	8- Sep- 2005	71° 00.41′ N	126° 04.46′ W	–	ADCP (92 m)	Technicap (102 m)	RCM11 (209 m)	Nichiyu (201 m)	397	2- Oct- 2006
CA05 (3rd year)	9- Sep- 2005	71° 16.84′ N	127° 32.18′ W	SBE37 (37 m)	–	–	–	–	211	2- Oct- 2006

Table 2
Number of MODIS images used to generate the multi-date surface POC composites presented in Fig. 4.

2004	05/30 to –06/14	06/15 to –06/29	06/30 to –07/14	07/15 to –07/29	07/30 to –08/15	08/16 to –09/02	09/03 to –09/21
Number of images	11	14	8	11	8	8	7
2005	05/31 to –06/15	06/16 to –06/29	06/30 to –07/15	07/16 to –07/29	07/30 to –08/14	08/15 to –09/01	09/02 to –09/17
Number of images	14	8	4	10	14	8	9
2006	05/29 to –06/13	06/14 to –06/28	06/29 to –07/14	07/15 to –07/28	07/30 to –08/13	08/14 to –08/31	09/01 to –09/18
Number of images	3	6	10	11	15	15	8

Images were selected when open water occupied an area $>10\%$ in the Amundsen Gulf region. Note that MODIS-Aqua has a daily coverage at 70°N.

phyto-detritus and fecal pellets (Forest et al., 2008a) that sink at speeds of 20–200 m d^{-1} (Turner, 2002); and (2) currents in the study area propagate at speeds of 5–10 cm s^{-1} and show opposite direction with depth (Ingram et al., 2008). Hence, we calculated that sinking particles should remain within a 5–50 km radius area before reaching 210 m depth.

2.3. Water column profiles, temperature sensors and current meters

A caged rosette-type oceanographic profiler equipped with a conductivity–temperature–depth system (CTD, Seabird SBE-911+) and a fluorometer (Seapoint) was deployed at mooring locations CA15, CA08 (~400 m isobath, 61 km from each other) and CA05 (211 m isobath, 28 km from CA15 and 57 km from CA08) during the CASES (October 2003 and July 2004) and ArcticNet expeditions (September 2005 and October 2006) on board the research icebreaker *CCGS Amundsen* (Fig. 1, Table 1). Temperatures were also recorded every 10 or 30 min in the surface layer (~35 m depth) using an Alec C/T probe or a Seabird SBE37 attached on moorings CA15 or CA05 from October 2003 to October 2006 (Fig. 1, Table 1). Unfortunately, the temperature probe deployed at ~35 m depth at CA08 in 2005–2006 did not produce any data. Hence, we decided to make use of the CA05 time-series to evaluate the inter-annual variability of temperature in the upper water column of the western Amundsen Gulf.

The CTD and moored T°-sensor data were calibrated and verified following the Unesco Technical Papers (Crease, 1988). Water samples were also taken on board for salinity calibration using a Guildline Autosal (resolution $<0.0002\pm0.002$). The fluorescence data were calibrated against *in situ* chlorophyll-*a* using the quadratic polynomial model of Tremblay et al. (2008) in 2003–2004 (r^2=0.91, n=124); and the linear regressions provided by J. Martin (Université Laval, Québec City, Canada) in 2005 (r^2=0.79, n=25) and 2006 (r^2=0.92, n=40). CTD and fluorescence data from all casts were averaged over 1-m bins. Calibrated surface layer temperatures (~35 m depth) from the moored T°-sensors were averaged over daily periods.

Oceanic circulation around the sediment traps were monitored every 20 or 30 min at CA15 and CA08 stations using current meters deployed at ~90 m (Acoustic Doppler Current Profilers, RDI-Teledyne instruments, first recording bin ~10 m above the instrument) and ~200 m depth (Aanderaa RCM-11 multi-sensors) (Fig. 1, Table 1). The pitch and roll measured by the ADCP at ~90 m depth were also used to estimate the tilt of the mooring line following the trigonometric relations given in Lee and Liu (2006). Processed current data were filtered using a 25 h low-pass filter to remove the weak (<0.5 m) diurnal and semi-diurnal tidal signals that prevail in the region (Kowalik and Proshutinsky, 1994; Ayles and Snow, 2002). Zonal and meridional current components were averaged over daily periods. Current velocities were also averaged over every trap sampling interval (see below) to test the effect of current speed on the magnitude of particle fluxes collected by the sediment traps.

2.4. Sequential sediment traps and vertical fluxes

Automated sediment traps were deployed at ~100 and ~210 m depth on moorings CA15 and CA08 (~400 m isobath, 61 km from each other) to collect settling particles continuously from October 2003 to September 2006 (Fig. 1, Table 1). The change of station from CA15 to CA08 in our study was the result of limited sample availability imposed by the combination of: (1) the malfunctioning of many sediment traps from 2003 to 2005 due to defective batteries and/or to a problem in the hardware used by the manufacturer; and (2) the logistical constraints and shortage of equipment when the mooring program was restructured in 2005 (i.e., at the transition between the CASES study and the new framework of the ArcticNet Observatory Network).

Two types of sequential traps were used in our study: (1) at ~100 m, a Technicap PPS 3/3 cylindrico-conical trap, with a 0.125 m^2 aperture, 12 cups, and an aspect ratio of 4.0; and (2) at ~210 m, a Nichiyu Giken Kogyo SMD26S-6000 conical trap, with a 0.5 m^2 aperture, 26 cups, and an aspect ratio of 1.5. The traps were programmed to collect particles synchronously in intervals of 7–30 days during the productive season (May–September) and in periods of 15–90 days during the other months. Both traps were equipped with baffled openings to reduce turbulence and retain deposited particles within collectors. Despite different designs and the fact that conical traps are known for their tendency to under-collect sinking particles (Buesseler et al., 2007), similar types of traps have proven successful for measuring comparable flux patterns in previous multi-year studies in Arctic waters (Hargrave et al., 2002; Sampei et al., 2004).

Sediment traps were prepared following the JGOFS protocols (Knap et al., 1996). Sample cups were filled with filtered seawater (Whatman glass fiber filters (GFF) 0.7 μm) adjusted to a salinity of 35 with NaCl. Formaldehyde was added as a preservative (5% v/v, sodium borate buffered). After retrieval, sample cups were put aside for 24 h to allow particles to settle. Zooplankton swimmers were removed from the samples with a 1-mm sieve and by hand-picking under a stereomicroscope (10–100X). Seasonal patterns in swimmers that accumulated in sample cups will be reported elsewhere, but the abundance of organisms was highest during late fall and winter when large calanoid copepods (>3 mm) were the dominant species. Few swimmer organisms were present in sample cups during the ice-reduced periods of ~May–October.

Sediment trap sub-samples were filtered in triplicate through pre-weighed GFF filters (25 mm, pre-combusted 6 h at 450 °C) for the determination of dry weight (DW), particulate organic carbon (POC) and particulate nitrogen (PN) fluxes. Filters were dried to constant weight for 12 h at 60 °C and weighed again for DW. After exposure for 12 h to concentrated HCl fumes to remove the inorganic carbon fraction, samples were analyzed on a Perkin-Elmer CHNS 2400 Series II to measure POC and PN (accuracy <0.3% and precision <0.2%). Mass flux (DW), POC and PN fluxes were expressed as daily fluxes (mg m^{-2} d^{-1}). The missing fluxes at the time of the mooring turnovers were calculated as the mean of the two contiguous values. The daily fluxes from October to December 2006, when no particle flux sampling was performed, were

estimated by using the averaged fluxes of 2003, 2004 and 2005 recorded during that period. Annual DW, POC and PN fluxes were calculated by summing each of the daily fluxes from January to December in 2004, 2005 and 2006. Organic carbon to nitrogen atomic mass ratios (C:N, molar) were determined using the POC and PN fluxes. Fluxes were not corrected for dissolution losses which were assumed to be constant among sample cups (Fischer et al., 1996; Hargrave et al., 2002). Hence, the particle fluxes should be regarded as minimal estimates in our study.

2.5. Relationships between vertical fluxes, current velocities and surface POC

The vertical mass fluxes and POC fluxes were related to the averaged current velocities recorded during each of the trap sampling intervals to evaluate the effect of currents on the collection efficiency of sediment traps. For the entire sampling period of 2003–2006, mass fluxes, POC fluxes and C:N ratios at 210 m depth were averaged to the same intervals as the 100 m values ($\geq$15 days) to verify the coherency between the two time-series. For each period from ~June to September, vertical POC fluxes, adjusted to the same semi-monthly time-windows as the satellite images, were related to remotely sensed surface POC concentrations extracted over the moorings to assess the relationship between surface POC pools and vertical POC fluxes. Only the surface POC values obtained with at least 10% of unmasked pixels were retained for these calculations. For the same time-windows, and only for the periods when the mooring site was in open water (i.e., defined as $>$10% of unmasked pixels within the 5 km radius area), POC fluxes at 210 m depth were related to the 100 m POC fluxes for a comparison with the relationships obtained between surface POC concentrations and the 210 m POC fluxes. All the linear regressions were tested using Pearson's correlation coefficient (significance level $\alpha < 0.05$) in order to take into account all the variables within each of the diverse ensembles.

3. Results

3.1. Sea ice, sea surface temperature and wind

From October 2003 to December 2006, the western Amundsen Gulf (Fig. 1) was characterized by recurrent first-year ice covers (Fig. 2). The timing of ice break-up in spring ($<$50% ice concentration), the extent of the reduced ice cover period and the various ice stages of development all exhibited marked inter-annual variability (Fig. 2, Table 3).

In 2004, ice concentration declined sharply from ~100% in May to a minimum of 8% by early August (Fig. 2). From late July to October 2004, old sea ice from the fragmenting central pack moved across the region, coinciding with strong winds ($\geq$40 km h^{-1}) from the west–northwest (Fig. 3). In 2005, the ice cover was already below 75% by mid-May in accordance with strong easterly winds ($\geq$40 km h^{-1}) that blew over the region during that month (Fig. 3). The duration of the ice-reduced season in 2005 ($<$50% ice concentration) was the longest out of the 3-year study (Table 3). In 2006, the western Amundsen Gulf remained covered by ice ($>$50%) until July (Fig. 2). As observed in 2004 and 2005, moderate to strong easterly winds dominated (23–55%) from May to July 2006 (Fig. 3). However, the dominance by easterlies (29–50%) persisted in August and September 2006, whereas frequent spells of strong winds from the west–northwest were recorded during late summer in both 2004 and 2005 (Fig. 3).

Every year, SST increased above 0 °C concomitantly to ice melt, peaked around 4–6 °C in late July/early August, and decreased then in agreement with the onset of the fall season in September (Fig. 2). The earliest increase (late May) and the longest period of warm SST (~15 weeks above 2 °C) were observed in 2005 in conjunction with a lengthened ice-reduced season. The seasonal mean of SST (average for the ice-reduced period of June–September) was also higher in 2005 than in 2004 and 2006 (Table 3).

3.2. Composite images of surface POC concentrations

The multi-date composite satellite images produced for the months of June–September in each of the years 2004–2005–2006 (Fig. 4) supported the variability of sea ice conditions observed in Amundsen Gulf (Fig. 2). In particular, the dark grey areas on the images were coherent with the 3-year cycle of ice concentration extracted from the CIS Ice Graph Tool, suggesting that masked pixels were essentially due to the presence of sea ice.

It is worth highlighting that in 2004 and 2005 the landfast ice bridge between Banks Island and Cape Parry formed during late winter, subsequently creating the typical pattern of the Cape Bathurst Polynya in spring (Fig. 4). A different situation occurred in 2006 when sea ice retreated first in the eastern Amundsen Gulf

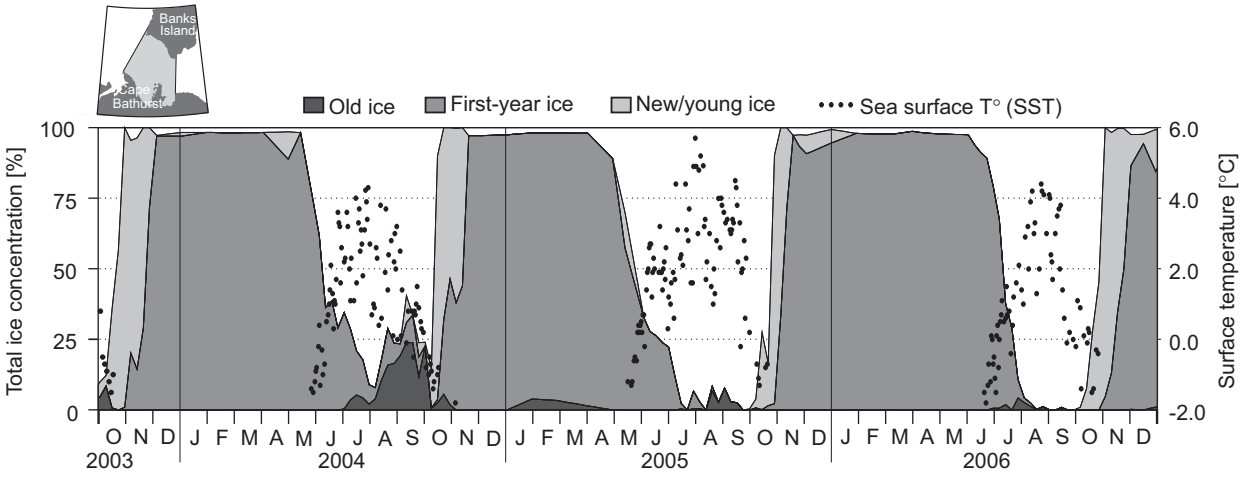

Fig. 2. Time-series of weekly sea ice concentration (% cover) divided into its various stages of development and daily MODIS-Aqua SST recorded over the western Amundsen Gulf from October 2003 to December 2006. The precise area over which sea ice and SST data were extracted in the Amundsen Gulf is shown above the panel.

Table 3
Annual variables recorded in the western Amundsen Gulf in 2004, 2005 and 2006.

Annual variable		2004	2005	2006
Timing of ice break-up (< 50% ice cover)		Early June	Late May	Early July
Number of days with < 50% ice coverage		126 days	154 days	112 days
Mean SST from MODIS (June–Sept.) (°C)		1.7 ± 0.2 (77)	2.5 ± 0.1 (82)	1.3 ± 0.2 (59)
Mean T° (°C) at 35 m depth (June–Sept.) (°C)		0.2 ± 0.1 (13968)	1.2 ± 0.1 (12336)	−1.4 ± 0.1 (16568)
Mean surface POC concentration over CA15 or CA08 in open water (mg POC m^{-3})	5 km	73.3 ± 3.6 (3)	64.6 ± 4.7 (7)	123.9 ± 13.9 (3)
	25 km	75.8 ± 4.2 (4)	65.4 ± 5.1 (6)	113.9 ± 17.4 (3)
	50 km	79.6 ± 5.3 (6)	67.8 ± 6.6 (7)	109.5 ± 25.2 (4)
Mean annual current velocity at CA15 or CA08 (cm s^{-1})	80 m	7.6 ± 0.1 (8736)	8.3 ± 0.1 (8592)	5.1 ± 0.1 (4771)
	200 m	4.5 ± 0.1 (6936)	4.9 ± 0.1 (8304)	2.4 ± 0.1 (4776)
Total mass flux at CA15 or CA08 (g DW m^{-2} yr^{-1})	100 m	36.3 ± 1.7 (7)	45.1 ± 0.6 (12)	64.5 ± 1.7 (11)
	210 m	17.2 ± 0.3 (14)	65.0 ± 0.8 (23)	24.0 ± 0.2 (21)
Total POC flux at CA15 or CA08 (g POC m^{-2} yr^{-1})	100 m	3.3 ± 0.1 (7)	4.2 ± 0.1 (12)	6.0 ± 0.1 (10)
	210 m	1.3 ± 0.1 (14)	2.2 ± 0.1 (21)	2.3 ± 0.1 (22)
Mean percent of POC in mass flux (%POC/DW)	100 m	10.4 ± 1.2 (7)	9.8 ± 0.6 (12)	13.1 ± 2.0 (10)
	210 m	7.6 ± 0.5 (14)	5.0 ± 0.6 (21)	12.6 ± 2.2 (22)
Mean C:N ratio of organic matter (a:a)	100 m	8.4 ± 0.3 (7)	8.1 ± 0.7 (12)	9.3 ± 1.1 (10)
	210 m	9.3 ± 0.5 (14)	8.9 ± 0.4 (21)	11.7 ± 1.5 (22)

The corresponding standard error and sample size (n) are also given for each of the parameters.

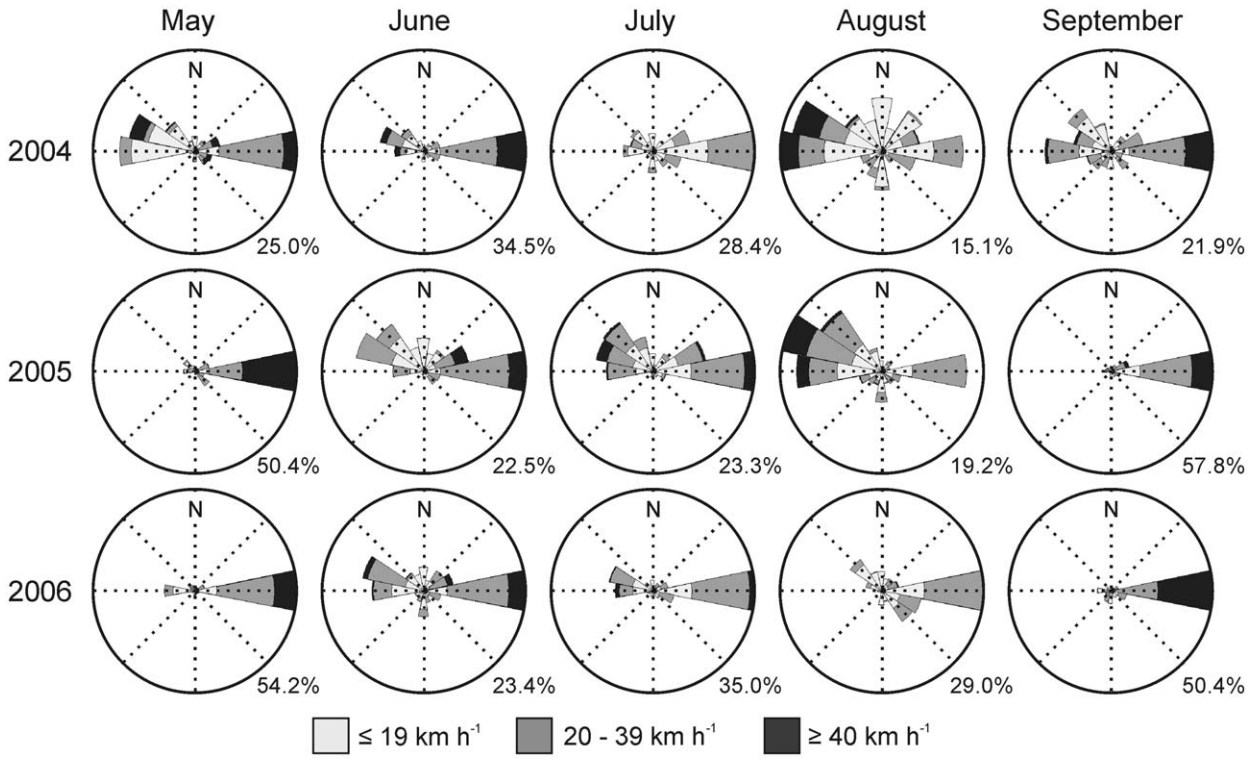

Fig. 3. Cumulated monthly wind roses recorded at Cape Parry (Fig. 1) during the open water period (~May–September) in 2004, 2005 and 2006. The percent frequency corresponding to the outer circle is given. The wind roses indicate the direction from where the wind was coming.

since the landfast ice bridge did not build up during the previous winter.

Each year following ice melt, increases in surface POC concentrations (> 100 mg C m^{-3}) occurred primarily in the shallow (< 200 m depth) southwestern Amundsen Gulf (Fig. 4). In June 2004, a thin plume of increased surface POC (~200 mg C m^{-3}) was observed in the prolongation of Cape Bathurst. One month later, surface POC reached ~300 mg C m^{-3} in Franklin and Darnley bays when landfast ice had disaggregated. Surface POC concentrations decreased afterward at the same time as old sea ice moved across the region in August 2004. In June 2005, a distinct patch of increased surface POC (200–400 mg C m^{-3}) was

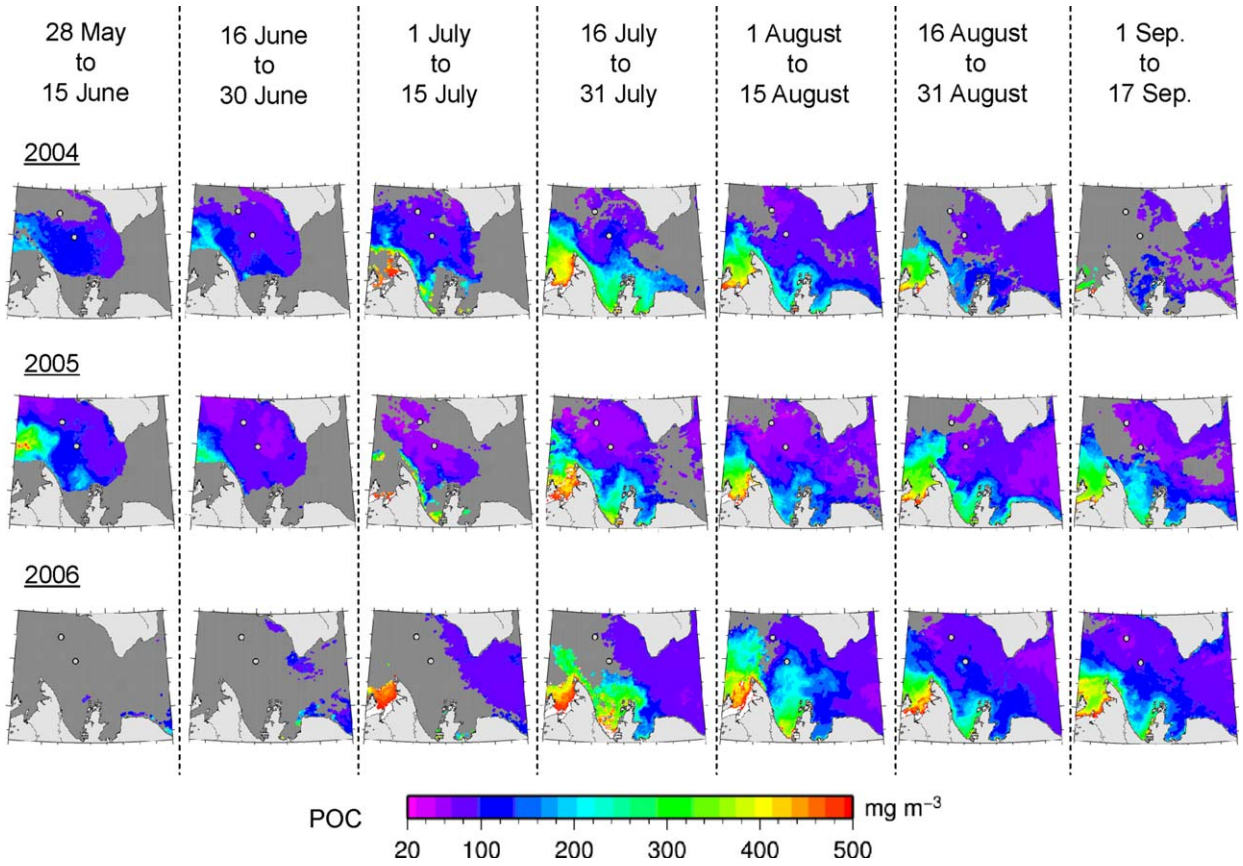

Fig. 4. Concentrations of POC in surface waters of the Amundsen Gulf from late May to September in 2004, 2005 and 2006 as derived from MODIS satellite data. The dark grey color corresponds to masked pixels due to the presence of sea ice or any other flags (see Section 3.2).

detected north of Cape Bathurst. From late July to September 2005, surface POC remained relatively high (200–300 mg C m^{-3}) in the southwestern Amundsen Gulf. In mid-July 2006, a rapid increase of surface POC (up to 500 mg C m^{-3}) was observed when sea ice retreated. Two weeks later, a plume of increased surface POC ($\sim$200 mg C m^{-3}) expanded over the moorings at the same time as the ice edge receded northward.

When extracted within circle areas of 5, 25 and 50 km radius over CA15 and CA08 during the open water weeks of 2004–2005–2006, semi-monthly POC concentrations estimated in the surface layer ranged from 50 to 150 mg C m^{-3} (results not shown). Linear regression of surface POC concentrations at CA08 against those measured at CA15 produced a significant ($\alpha < 0.05$) one-to-one relationship (y=1.08x+4.07, r=0.78, $p < 0.01$, n=48). On a seasonal basis, the greatest mean surface POC concentration (averaged values for the entire June–September period within each of the three distinct areas) was recorded in 2006, followed by 2004, and then by 2005 (Table 3).

3.3. *Water column profiles, surface layer temperature and current vectors*

The temperature and salinity (T/S) profiles recorded at the time of mooring deployments or recoveries (Table 1) were consistent with the layering of water masses previously reported for the Beaufort Sea: the Polar-Mixed Layer overlaid on the Pacific Halocline which itself overlaid Atlantic Waters (Fig. 5a and b). As expected, most of the seasonal T/S variability (-1.5 to 3 °C/salinity of 26–32) occurred near the surface. Based on the vertical T/S profiles, the bottom limit of the stratified surface layer was located at 40–45 m depth in the western Amundsen Gulf (Fig. 5a and b). The sediment traps deployed at $\sim$100 and $\sim$210 m depth were moored within the Pacific Halocline where T/S properties did not vary much (-1.0 to -0.5 °C/salinity of 32–33). The fluorescence signal recorded during the CTD casts performed at mooring sites revealed the presence of a subsurface chlorophyll maximum ($\sim$0.8–1.6 μg Chl-a L^{-1}) in the lower part of the Polar-Mixed Layer (between 25 and 50 m) throughout the 3 years of the study (Fig. 5c).

From October 2003 to September 2006, temperature monitored in the upper water column ($\sim$35 m depth) at CA15 and CA05 was invariably cold during the fall and winter months (~ -1.0 °C), but exhibited distinct inter-annual patterns during the ice-reduced periods (Fig. 6a, Table 3). In 2004, temperature increased up to $\sim$2.0 °C from June to July and decreased sharply in August when old sea ice moved across the region. Temperature in 2005 started to increase in late May, reached a maximum of $\sim$4.0 °C in July and persisted above 0 °C until late September. In contrast, surface layer temperature in 2006 remained below 0 °C throughout the year (Fig. 6a).

Intensity and direction of the water flow recorded around the sediment traps varied markedly over the 3-year sampling period (Fig. 6b and c). Seasonal variations in current directions were similar at both depths, but velocities were generally two-times lower at 200 than at 80 m depth (Table 3). From October 2003 to February 2004, circulation was dominated by strong northward currents (up to $\sim$50 cm s^{-1}). Currents for the rest of 2004 were generally lower than 10 cm s^{-1}, except for episodic acceleration up to $\sim$20 cm s^{-1} in March, July and October. Strong southward currents (up to $\sim$40 cm s^{-1}) were recorded during the summer and fall of 2005. Circulation was invariably weak (< 12 cm s^{-1}) at

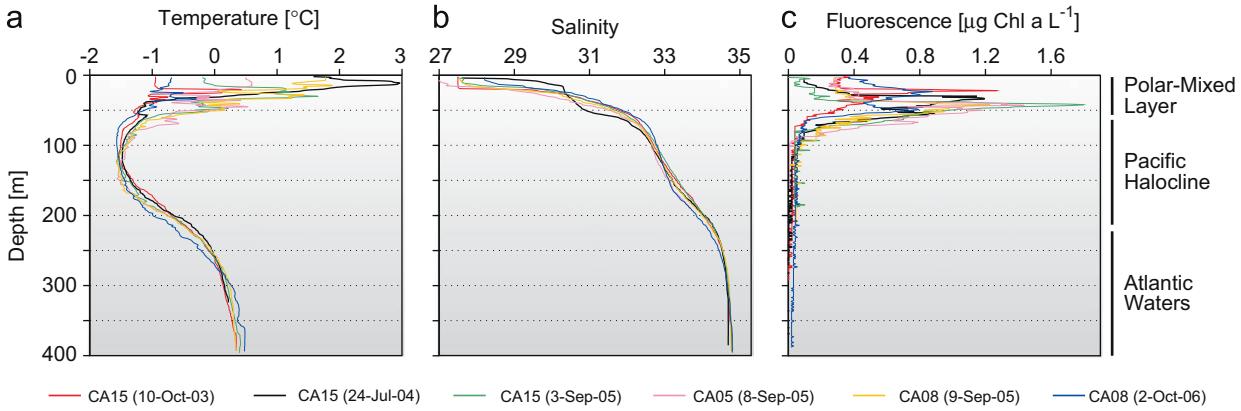

Fig. 5. Temperature–, salinity– and fluorescence–depth profiles conducted at mooring locations (Fig. 1) at the time of their deployment or recovery (see Table 1). The three main water layers present in southern Beaufort Sea are also identified on the right.

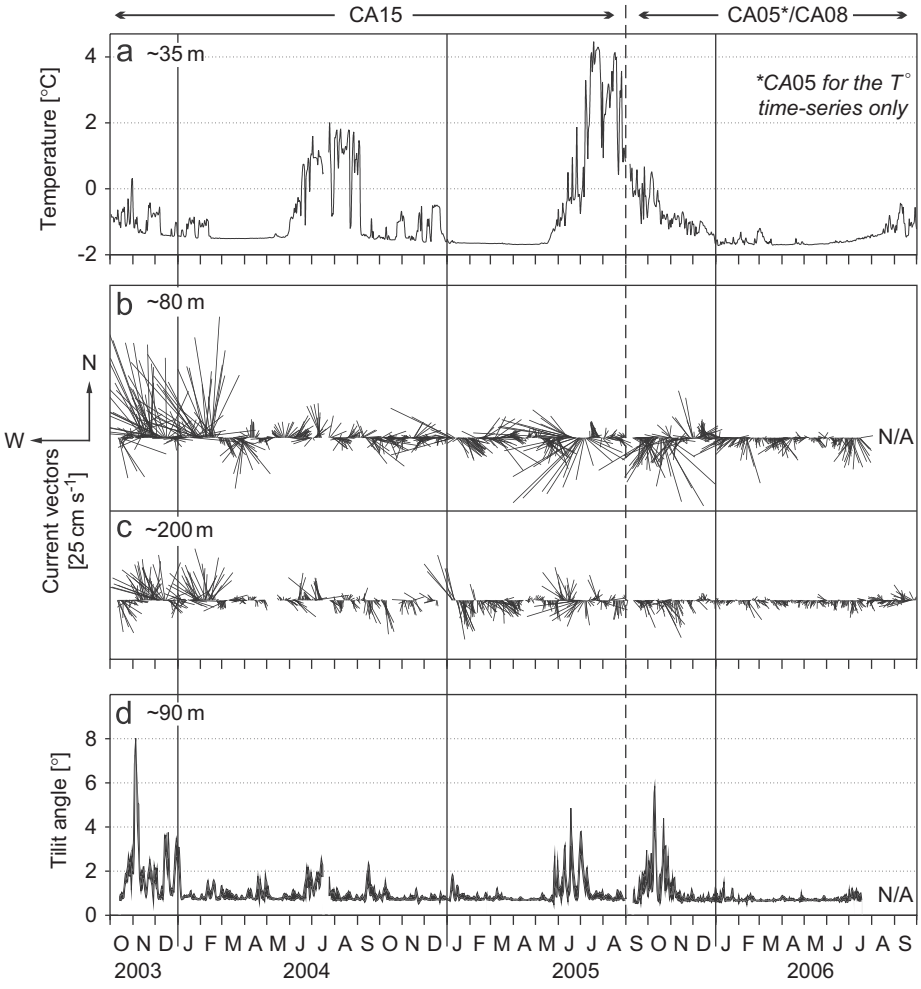

Fig. 6. Time-series of (a) temperature recorded at ~35 m depth at moorings CA15 and CA05; (b, c) daily low-pass filtered current vectors recorded at ~80 and ~200 m depth (close to the sediment trap depths) at CA15 and CA08; and (d) tilt range of the mooring line as calculated from the ADCP deployed at ~90 m depth at CA15 and CA08. The location of the moorings is given in Fig. 1 and details of the deployments in Table 1.

both depths throughout 2006. Except for episodic increases up to 4–8° in concomitance with current speeds $>30\,cm\,s^{-1}$, the tilt angle (drag) of the mooring line calculated at 90 m depth was particularly stable ($<2°$) throughout the 2003–2006 period (Fig. 6d). Overall, the linear relationship of tilt angles at 90 m against current velocities at 80 m depth was significant but weak (r=0.31, $p<0.01$, n=992) (result not shown).

3.4. Vertical fluxes of particle mass and POC

From October 2003 to September 2006, the POC content of vertical mass fluxes recorded over the 400 m isobath in the western Amundsen Gulf varied from 7% to 28% of total mass at 100 m, and from 2% to 35% at 210 m depth (Fig. 7a and b). The annual mass flux was higher at 100 than at 210 m depth in both

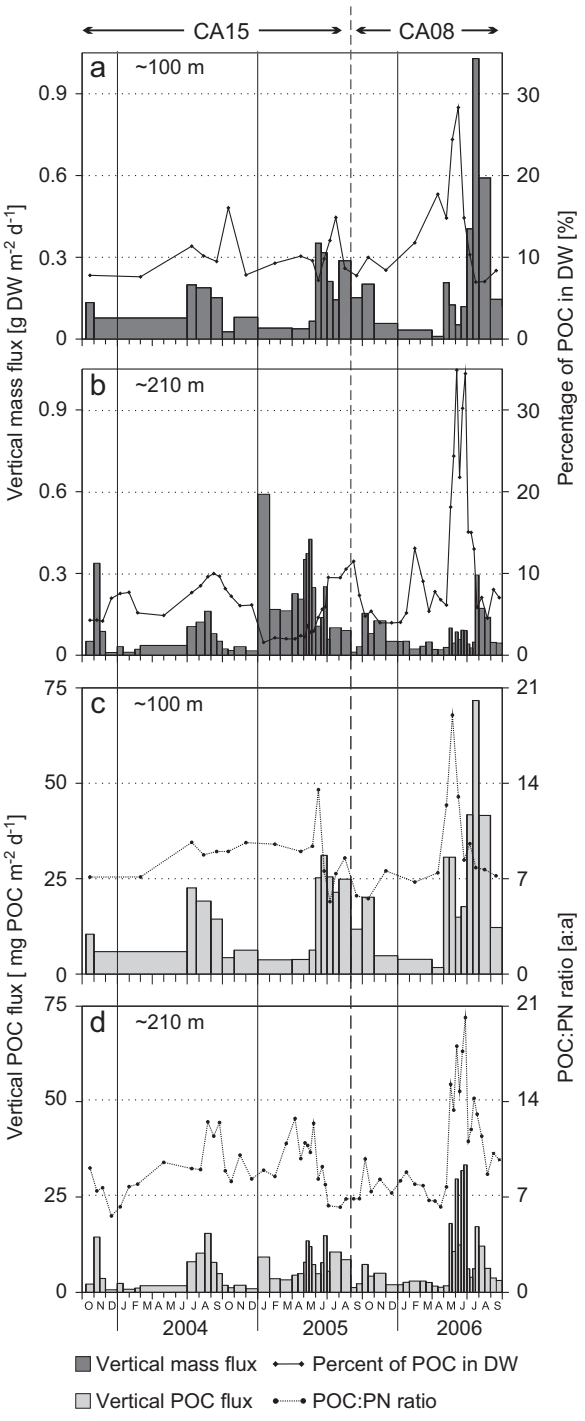

Fig. 7. Time-series of (a, b) daily vertical mass fluxes (dry weight, DW) and (c, d) particulate organic carbon fluxes (POC) recorded at ~100 and ~210 m depth in the western Amundsen Gulf (moorings CA15 and CA08) from October 2003 to September 2006. The corresponding percentage of POC in total DW and the C:N ratio of particulate organic matter for each sediment trap sample are also depicted as a line over the vertical mass fluxes and POC fluxes, respectively.

2004 and 2006, while it was higher at 210 than at 100 m depth in 2005 (Table 3). The 12-month averages of POC percentage were, however, constantly higher at 100 than at 210 m depth (Table 3). Each year, increases of POC content in mass flux (> 10%) occurred during the period of reduced ice cover (~May–October), although the maximum POC percentage was recorded at both depths from May to July 2006 when sea ice was still covering the mooring location (Fig. 4). Under ice cover, the fractions of POC in mass fluxes were generally lower than 10%. The lowest POC contents at 210 m depth were recorded in January–April 2005 when the highest mass fluxes (up to 0.6 g m^{-2} d^{-1}) were detected.

The time-series of vertical POC fluxes recorded at 100 and 210 m depth were characterized by distinct patterns of magnitude and temporal variability (Fig. 7c and d). When summed over 12 months, annual POC fluxes yielded maximum values in 2006, intermediate values in 2005 and lowest values in 2004 (Table 3), following the variability of daily POC fluxes during the ice-reduced periods (Fig. 7c and d). In 2004, a period of increased POC fluxes was recorded from July to September (up to 22 and 16 mg C m^{-2} d^{-1}, respectively, at 100 and 210 m depth). The averaged rates recorded at both depths in winter–spring 2004 are related to malfunctions in the trap's hardware or power supply. Unfortunately, the motor did not turn during this period. At mid-May 2005, a short rise (< 2 weeks) in the POC flux (up to 14 mg C m^{-2} d^{-1}) was recorded at 210 m depth (Fig. 7d). In 2005, a period of increased POC fluxes occurred from June to October (up to 31 and 15 mg C m^{-2} d^{-1}, respectively, at 100 and 210 m depth). During this period, the peak fluxes were recorded at both depths in late June, following the development of enhanced surface POC concentrations (200–400 mg C m^{-3}) north of Cape Bathurst (Fig. 4). In 2006, a period of elevated POC fluxes occurred from May to early September (up to 72 and 33 mg C m^{-2} d^{-1}, respectively, at 100 and 210 m depth). At 100 m depth, two discrete maxima can be distinguished during this period: the first in May (31 mg C m^{-2} d^{-1}) when sea ice was still covering the region, and the second in late July (72 mg C m^{-2} d^{-1}) when increased surface POC (~200 mg C m^{-3}) expanded over the mooring location (Fig. 4).

From October 2003 to September 2006, the C:N ratios of organic matter fluxes generally oscillated between 6 and 9, and averaged higher annual values at 210 than at 100 m depth (Fig. 7c and d; Table 3). Increases of C:N ratios above 10 were recorded in August–September 2004 when old sea ice was detected in the western Amundsen Gulf, and in spring 2005 and 2006 when the first-year ice cover was still present (Fig. 2). The maximum C:N ratios were recorded in June 2006 (up to ~20), coincident with a percentage of POC in mass fluxes up to ~30%.

3.5. Relationships between vertical fluxes, current velocities and surface POC

Linear regressions of vertical particle fluxes against current velocities showed no significant trend (level of significance $\alpha < 0.05$), suggesting that hydrodynamic processes did not impact the measurement of trap-collected particle fluxes (Fig. 8). However, while this was clear for vertical mass fluxes at both depths and POC fluxes at 100 m ($p > 0.35$; Fig. 8a–c), the trend between current velocities at 200 m and POC fluxes at 210 m depth would have been significantly negative ($r = -0.22$, $p = 0.09$) if a level of significance $\alpha < 0.1$ had been chosen (Fig. 8d).

The regressions of mass fluxes and POC fluxes at 210 m depth against the 100 m values for the entire sampling period of 2003–2006 exhibited parallel trends lower than a 1:2 proportion (Fig. 9a and b), but no significant relationship ($\alpha < 0.05$) was detected ($r < 0.3$, $p > 0.1$). Interestingly, the 210 m anomalies of mass fluxes (January–April 2005) and POC fluxes (June 2006) did not correspond to the same samples. A significant relationship was calculated ($r = 0.54$, $p < 0.01$) between the two C:N time-series, within which one outlier corresponded to June 2006 (Fig. 9c).

During the open water periods of 2004, 2005 and 2006, daily-adjusted POC fluxes recorded at 100 m depth correlated significantly ($\alpha < 0.05$) with surface POC concentrations extracted

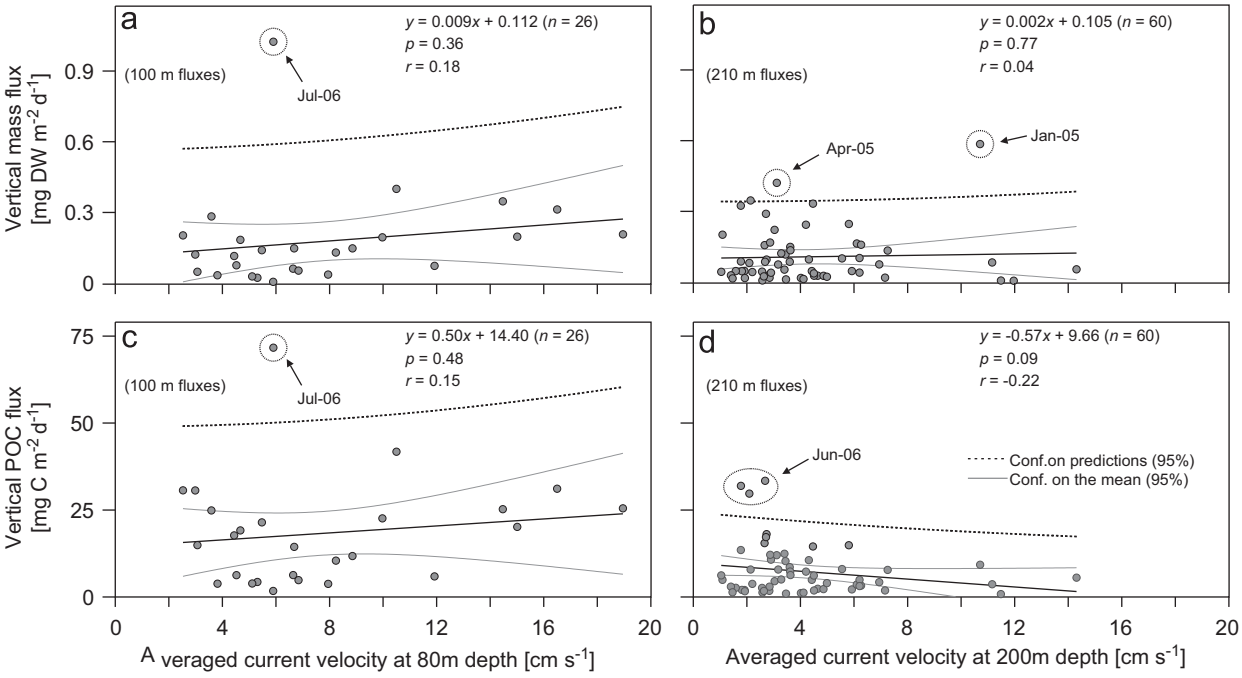

Fig. 8. Linear regressions of (a, b) vertical mass fluxes and (c, d) vertical POC fluxes recorded at ~100 and ~210 m depth at moorings CA15 and CA08 against current velocities monitored at the same moorings at ~80 and ~200 m depth, respectively. Current velocities were averaged over every trap sampling interval to evaluate the effect of current speed on the magnitude of particle fluxes collected by the sediment traps.

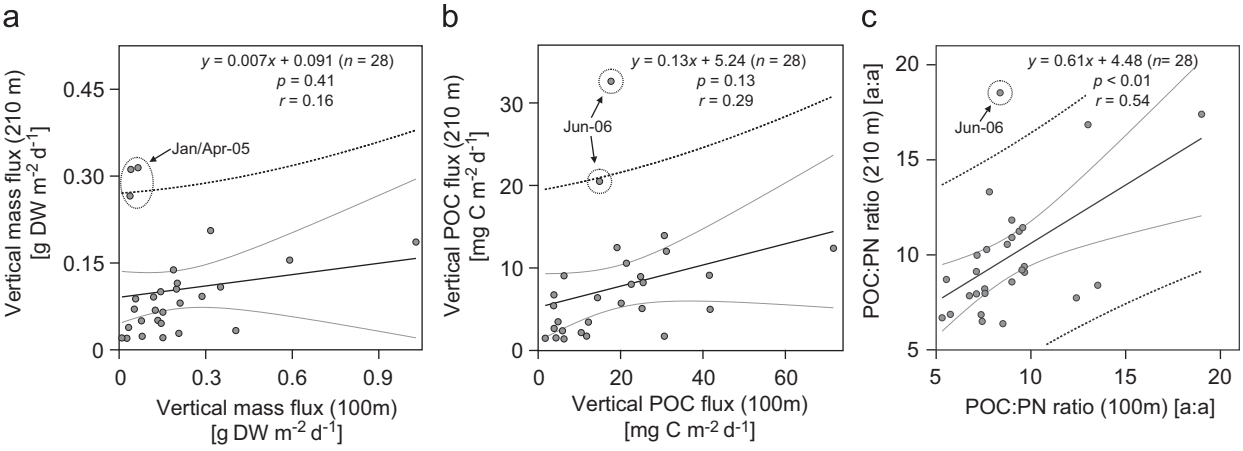

Fig. 9. Linear regressions of (a) vertical mass fluxes, (b) vertical POC fluxes and (c) C:N ratios recorded at 210 m depth against the 100 m values for the entire sampling period of 2003–2006. The high-resolution data recorded at 210 m depth (26-cup trap) were averaged to the same intervals as the 100 m time-series (12-cup trap) for the purpose of the regressions.

within circle areas of 5, 25 and 50 km radius ($r > 0.52$, $p < 0.05$) (Fig. 10a–c). The relations between surface POC and the fluxes at 100 m depth were, however, clearly forced by the data from the year 2006 when surface POC $> 100\,mg\,m^{-3}$ and POC fluxes $> 40\,mg\,m^{-2}\,d^{-1}$ were measured. These significant trends disappear ($r < 0.38$, $p > 0.32$; mean slope ≈ 0.10) when the data of 2006 are removed from the calculations (Fig. 10d, regression for the 5 km radius area showed as an example). No relationship ($r < 0.3$, $p > 0.1$) between vertical POC fluxes at 210 m depth and surface POC concentrations across all three radial areas was found (Fig. 10e–g). When using only the data when the mooring site was in open water, the regression of daily-adjusted POC fluxes at 210 m depth against the 100 m values produced a significant correlation (r=0.63, p=0.03) (Fig. 10h) that was still present if the fluxes from 2006 were removed (y=0.40x–1.77, r=0.74, p=0.02, n=9) (result not shown).

4. Discussion

We made use of distinct time-series recorded at moorings CA15 (2003–2005) and CA08/CA05 (2005–2006) to evaluate the influence of environmental variables on the seasonal and inter-annual variability of vertical POC fluxes in the western Amundsen Gulf. Temporal variability is supposed to exceed spatial variability in the Amundsen Gulf region (Arrigo and van Dijken, 2004) as well as in other Arctic polynya systems (e.g., Hargrave et al., 2002). But since the moorings were ca. 30–60 km from each other, we have to take into account a certain degree of spatial heterogeneity in our interpretation of differences in the timing and intensity of POC fluxes and their associated forcings. However, we assume that this heterogeneity was minimal because the physical and biological regimes in the area should affect the mooring sites by the same amount. First, the water column profiles and the current vectors

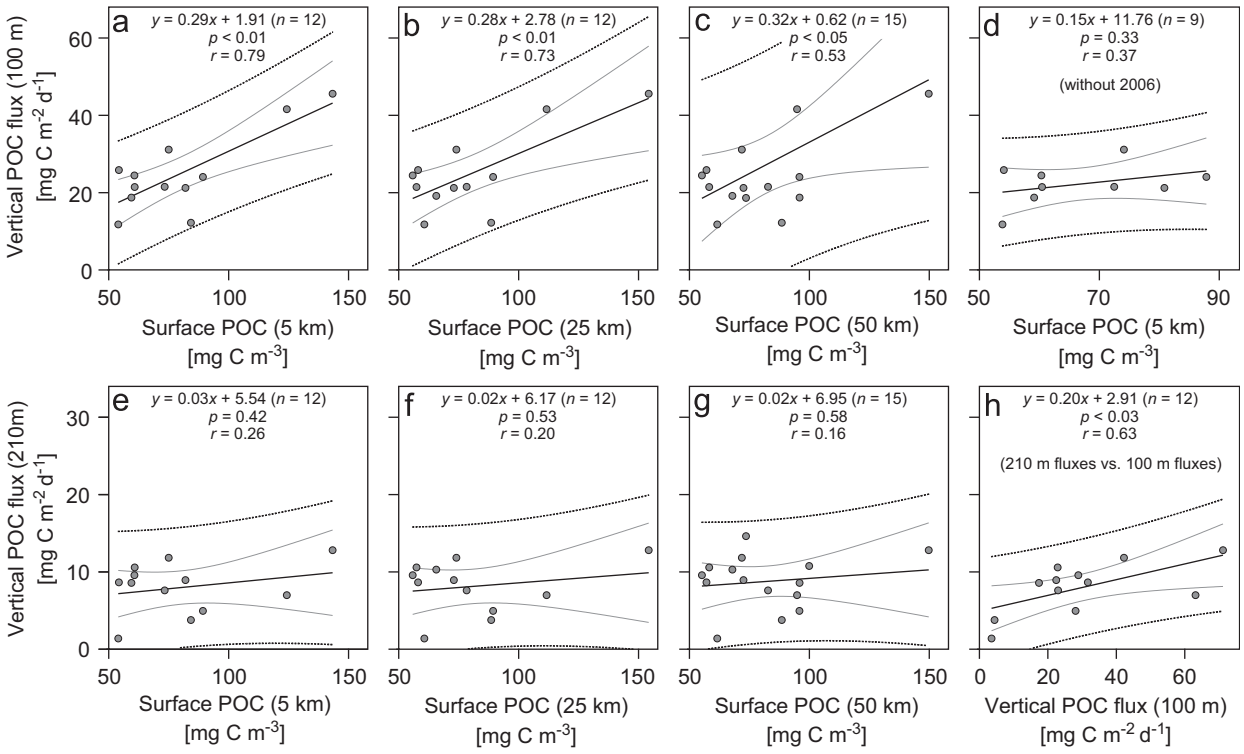

Fig. 10. Linear regressions of (a–g) period-adjusted vertical POC fluxes recorded in the western Amundsen Gulf against surface POC concentrations extracted over the sediment trap site as derived from MODIS images obtained during the open water season (June–September) in 2004, 2005 and 2006 (Fig. 4). Panels (a), (b) and (c) present the relations between the 100 m fluxes and the surface POC averaged over circle areas of 5, 25 and 50 km radius, respectively. Panel (d) is the regression of the 100 m fluxes using only the 2004–2005 data against surface POC within the 5 km radius area (as an example to show the absence of relation when the data of 2006 are removed). Panels (e), (f) and (g) show the regressions between the 210 m fluxes and the surface POC concentrations over circle areas of 5, 25 and 50 km radius, respectively. The last panel (h) is the correlation between the 210 m fluxes against the 100 m fluxes for the open water period only (defined as $>10\%$ of unmasked pixels within the 5 km radius area).

showed consistent patterns among the stations, suggesting that a same oceanographic setting prevails in the Amundsen Gulf. Second, ice conditions over the moorings were comparable from one satellite image to another and surface POC concentrations over both sediment trap sites correlated linearly ($\sim$1:1). Third, the two trap sites were located at the same distance ($\sim$70 km) from the edge of the Mackenzie Shelf (60–80 m isobath). This implies that material transported from the shelf would affect particle fluxes over the ca. 400 m isobath to the same extent. Finally, both mesozooplankton and macrobenthos assemblages were previously determined as being statistically similar over bottom depths >250 m in the area (Darnis et al., 2008; Conlan et al., 2008). This supports furthermore our assumption that the two mooring sites where vertical fluxes were collected are ecologically similar. Therefore, we conclude that the use of different stations to investigate the temporal variability of POC fluxes in the western Amundsen Gulf was adequate.

4.1. Seasonal variations and the origin of vertical POC fluxes in the western Amundsen Gulf

The seasonal changes in the nature and magnitude of vertical particle fluxes in the southeastern Beaufort Sea have been thoroughly examined by the use of moored sediment traps in recent studies (O'Brien et al., 2006; Forest et al., 2007, 2008a). Briefly, the annual cycle of downward POC fluxes can be divided into four different periods in relation to sea ice conditions: (1) under ice cover, when POC fluxes are low and dominated by resuspended detritus of mixed origin; (2) at vernal ice melt, when ice algae and exopolymers with high C:N ratios are quickly released to depth; (3) in open water, when POC fluxes are high and derive from autochthonous pelagic production; and (4) at ice freeze-up, when shelf bottom POC with a substantial terrigenous fraction is advected offshore. Over our 3-year study, the distinct time-series of settling particles were in general agreement with this sequence. In particular, the recurrent increase of POC content in mass fluxes, C:N ratios and POC fluxes between $\sim$May and October illustrated that biological activities (i.e., photosynthesis and zooplankton feeding) were most likely the main determinants of the seasonal variability of downward POC fluxes in the western Amundsen Gulf.

In the present work, local resuspension was not supposed to affect sediment traps moored ≥ 200 m above the seafloor. But lateral transport of particles resuspended elsewhere (e.g., on the shelf) may potentially contribute to vertical POC fluxes at the mouth of Amundsen Gulf. This is mostly true for particle fluxes collected in late fall and winter, since autumnal storms and thermohaline convection on the shelf are efficient processes for advecting the benthic nepheloid layer ($\sim$20 m thick) offshore (Backhaus et al., 1997; O'Brien et al., 2006; Mucci et al., 2008). Current surges and inversions, eroding the shelf-break of the Mackenzie Shelf ($\sim$80 m isobath), are also recurrent features found under ice cover conditions (Forest et al., 2007, 2008b). Here, the positive mass flux anomalies recorded at 210 m depth from January to April 2005 can be directly linked to an energetic water pulse ($\sim 100\,\mathrm{cm\,s^{-1}}$) that generated massive resuspension and particle dispersal across the shelf-break (see Forest et al., 2008b for details). However, the POC content of such particle fluxes is usually weak (1–8%); and most of the particles within intermediate nepheloid layers appear to sink rapidly over bottom depths <300 m (Forest et al., 2007; Mucci et al., 2008). Hence, in

our study, the increase of vertical POC fluxes induced by the above mechanisms is less apparent when compared to the spring–summer maxima that probably originate from biological production. Thus, we assume that intermittent detachments of nepheloid layers into the mid-water column off the shelf-break fed particle fluxes during the late fall and winter months only, and mainly at 210 m depth.

The more positive $\delta^{13}C$ and $\delta^{15}N$ signatures (i.e., marine source) of surface seabed sediments in the Amundsen Gulf, compared to values obtained on the Mackenzie Shelf/Slope, suggest that terrigenous material is a minor constituent of vertical particle fluxes over the $\geq$400 m isobath in southeastern Beaufort Sea (Morata et al., 2008; Mucci et al., 2008). In addition, results from the Canadian Arctic Shelf Exchange Study (CASES), based on the aluminum content of trap-collected particles (O'Brien et al., 2006), revealed that terrigenous inputs accounted for ~5% of vertical POC fluxes at 100 and 200 m depth in 2003–2004 in the central Amundsen Gulf (1.2–3.4 g C m^{-2} yr^{-1}) (Sasaki et al., 2006). By contrast, downward POC fluxes measured at similar depths at the edges of the Mackenzie Shelf in 1987–1988 and 2003–2004 (1.0–5.8 g C m^{-2} yr^{-1}) had a substantial terrestrial POC fraction (10–35%) in relation to the transport of shelf bottom material, river particles or coastal erosion (O'Brien et al., 2006; Forest et al., 2007, 2008a). These observations diverge from Amiel and Cochran (2008) who combined ^{234}Th and $\delta^{13}C$ measurements in June–July 2004 to estimate that terrigenous POC fluxes were 4- to 10-fold higher than marine POC fluxes both on the Mackenzie Shelf/Slope and in the Amundsen Gulf. This discrepancy is probably due to a too positive $\delta^{13}C$ marine end-member employed in their work with respect to the study area (see Stein and Macdonald, 2004).

In our 3-year study, we therefore assume a dominance of shelf sediment supply during late fall/winter and a 5% of terrigenous inputs in spring–summer. This enables us to estimate the fraction of downward POC fluxes likely attributable to the 'algal pathway', which proceeds by the sinking of newly produced POC at or next to ice break-up (*sensu* Forest et al., 2008a). These fluxes were estimated in 2004, 2005 and 2006, respectively, to be 79%, 75% and 84% of annual POC fluxes at 100 m (i.e., 2.6, 3.2 and 5.0 g C m^{-2} yr^{-1}), and to be 64%, 61% and 75% of fluxes at 210 m depth (i.e., 0.8, 1.3 and 1.7 g C m^{-2} yr^{-1}). Thus, the majority of settling POC collected in the western Amundsen Gulf over our study was the result of the autochthonous processes (i.e., marine source) that occurred during ice melt or in open water.

4.2. Sea ice regime and the contribution of ice-released material to vertical POC fluxes

Over our 3-year study, sea ice conditions in the Amundsen Gulf were within the breadth of the sea ice climatology (1980–2004) reported by Galley et al. (2008). With an ice break-up ($<$50% ice concentration) in early June, the year 2004 may be considered as normal, but the significant presence of old ice in summer followed a positive trend in multi-year sea ice (1–2.5% per year) observed west of Banks Island over the previous 25 years. This trend in old ice reaching into the mouth of the Amundsen Gulf is due to increased cyclonic motion in the central pack and has been attributed to differential reduction in perennial sea ice between the eastern and the western Arctic (see Galley et al., 2008). Few fragmented multi-year sea ice was observed in the summers of 2005 and 2006, suggesting that the increasing trend probably came to an end in 2004. In our work, the earliest ice break-up, the warmest surface temperatures and the longest ice-free season all occurred in 2005. This year was associated with a global warming anomaly (land and ocean combined; +0.61 °C), higher than in 2004 and 2006, and preferentially observed in the northern regions (NCDC, 2009). A record low extent of Arctic sea ice, compared to the minimum ice extents of September over the period 1979–2006, was also recorded in 2005 (Serreze et al., 2007). The ice regime in the Amundsen Gulf behaved differently in 2006 than in 2004 and 2005. The landfast ice bridge connecting Banks Island to the continent did not build up in late winter 2006 and the summer retreat of sea ice nearby Cape Bathurst was delayed until July. While these conditions contrast with 2004 and 2005, this discrepancy is not unusual since the fast ice bridge only formed once in every 3 years in the previous 25 years (CIS, 2007).

The first component of vertical POC fluxes affected by the variability of sea ice conditions in spring–summer should be the contribution of biogenic particles retained by the ice cover such as ice algae (e.g., Renaud et al., 2007) and exopolymeric substances (e.g., Riedel et al., 2006). By using microscopic, isotopic and elemental analyses, Forest et al. (2007) demonstrated that vertical POC fluxes derived from ice algae and exopolymers can be identified when an elevated percentage of POC in mass flux (15–25%) and high C:N ratios (14–21) are synchronized with ice break-up. This counter-intuitive connection between 'fresh' algal particles and high C:N ratios is explained by the sinking of ice diatoms aggregated with the viscous exopolymers they produce (C:N $\approx$ 20; Engel and Passow, 2001). Time-series of sinking particles collected at 1, 15 and 25 m depth under the landfast ice of Franklin Bay in spring 2004 also showed increasing C:N ratios (up to 12) in response to the release of organic particulate material from ice cover melt (Juul-Pedersen et al., 2008). Furthermore, Meiners et al. (2003) observed an increase in the C:N ratio of ice-retained particles, from young (~6) to first-year (~12) and multi-year (~17) sea ice, in association with an increasing content of ice pennate diatoms and exopolymer particles.

In the present study, indications of vertical POC inputs from sea ice communities were primarily detected at vernal melt in 2005 and 2006. In particular, the ice-related POC maxima of May–June 2006 were relatively high as the ice cover persisted over the mooring in spring, allowing epontic algae to develop within the first-year ice matrix during a period of increased irradiance (e.g., Michel et al., 2006). Despite a noticeable ice algae signature seen in May 2005, the magnitude of associated POC fluxes was not as high as in 2006 since the ice cover melted 6 weeks earlier in 2005. No ice-released POC was detected at spring melt 2004, probably because the brief ice algae signal has been diluted into the averaged flux values of winter–spring when the trap carousels did not turn. However, the increase of C:N ratios, concurrent with the apparition of old ice in late summer 2004, suggests that ice-retained particles contributed to some extent to vertical fluxes during this period. Hence, we propose that the melt of first-year/old sea ice may supply occasional pulses of ice algae and/or exopolymers up to 210 m depth in the Amundsen Gulf. In addition, we surmise that the rapidly exported 'fresh' POC from vernal ice melt (Renaud et al., 2007; Forest et al., 2007) would provide a key food resource for the benthic organisms that survive over the $\geq$400 m isobath (e.g., Bessière et al., 2007; Conlan et al., 2008).

4.3. Pelagic production and the inter-annual variability of surface POC pools and fluxes

Although episodic inputs of ice algae contribute to vertical POC fluxes in Arctic seas, the bulk of particulate organic matter exported from the surface layer during the ice-reduced season is derived from pelagic primary production (e.g., Forest et al., 2008a; Tamelander et al., 2008; Reigstad et al., 2008). In our work, the most intense vertical POC export was recorded in late July 2006, that is, just following the retreat of the ice cover during a year of late ice

break-up. Interestingly, POC fluxes during the warm summer 2005 were lower than in 2006, and were lowest in 2004 when old ice moved across the region in August–September. In an attempt to understand the inter-annual variability of POC pathways in the Amundsen Gulf, the contrasting scenarios presented by Bluhm and Gradinger (2008) may provide a good conceptual framework (see their Fig. 4). The basic premise of their model is that, in years of late ice break-up (and thereby, low seasonal surface temperature), the ice algae seed the spring bloom that starts rapidly at the ice edge. In contrast, in years with early ice break-up, the bloom occurs in relatively warm open waters and is not associated with the ice edge. These scenarios also suggest that in warm years, zooplankton production is higher than in years of abundant ice and that more POC flows into the pelagic networks, while zooplankton has less grazing impact in cold years when the ice retreats late, and that POC is predominately exported to the benthos (see also Loeng et al., 2005).

Out of the 3 years studied here, 2005 and 2006 may be relevantly interpreted in the context of this conceptual framework. During 2006, sea ice broke up late in July and sub-zero temperatures in the upper water column persisted in summer. On the satellite images, a zone of increased POC concentrations ($>200\,mg\,m^{-3}$) was observed along the ice margin as soon as it receded northward in late July–early August. Hence, we link this expansion of elevated surface POC to the rapid development of an ice edge bloom probably inoculated by ice algae (e.g., Jin et al., 2007). Since primary production in 2006 would have been less vulnerable to zooplankton control when it develops in cold waters (Bluhm and Gradinger, 2008), the surface POC that expanded over the mooring might have been preferentially exported to depth. In contrast, sea ice melted early in 2005 and surface POC reached the lowest concentrations ($<50\,mg\,m^{-3}$) recorded throughout our study. The suppression of the surface POC pool by micro/mesozooplankton grazing during the warm year 2005 is a possible cause for the reduced amount of detectable POC (e.g., Banse and English, 1999; Venables et al., 2007). Nevertheless, the patch of increased POC observed over the Mackenzie Shelf in June 2005 suggests the development of a phytoplankton bloom confined to this area. We associate the elevated POC concentrations to phytoplankton production since the Mackenzie River plume does not expand over the outer shelf when the freshet is still constrained by ice in close proximity to coast, as seen in early June (Carmack and MacDonald, 2002; O'Brien et al., 2006; Emmerton et al., 2008). A potential explanation for such a geographically limited bloom is the combination in spring 2005 of dominant easterly winds and ice-free waters beyond the shelf-break that could have induced on-shelf upwelling of deep nutrients (Carmack and Chapman, 2003). However, the lack of zooplankton and nutrient data during the springs and summers of 2005 and 2006 prevents any confirmation of the hypotheses listed above.

When compared to 2005 and 2006, the surface POC concentrations measured in 2004 are better connected to the *in situ* results of the recent CASES program. In spring–summer 2004, the new phytoplankton production inferred from nutrient drawdown was weak ($\sim18\,g\,C\,m^{-2}\,d^{-1}$) and developed mainly in association with the nutricline at depth (Tremblay et al., 2008). This low POC production has been explained by the weakness of physical mixing processes during the preceding fall and winter, which prevented any homogenization of the surface layer with the nutrient-rich deep waters (Tremblay et al., 2008; Simpson et al., 2008). And by limiting light availability, the increasing presence of old sea ice in late summer most probably prevented any extensive primary production in 2004. Moreover, the large calanoid copepods, which dominate (>70%) the zooplankton biomass in southern Beaufort Sea (Darnis et al., 2008), were intensely grazing on the weak phytoplankton production (Seuthe et al., 2007; Forest et al., 2008a). The integrated bacterial production measured in the upper 220 m in the Franklin Bay from late June to August was also relatively high ($\sim2.3\,g\,C\,m^{-2}$; Garneau et al., 2008), corresponding then to ~13% of the new primary production. Hence, we conclude that vertical POC fluxes in 2004 were the lowest out of our 3-year study as a result of low primary production, continuous top-down control by herbivorous copepods and efficient recycling by microbes.

The distinct patterns of algal blooms (or absence thereof) observed in our study thus support the striking inter-annual variability of primary production reported by Arrigo and van Dijken (2004) for the Amundsen Gulf. However, uncertainties remain about how much exactly of the whole surface POC pool the satellite sensor was able to capture. Typically, remote sensing captures the first few meters below the surface, but this range can be extended to several tens of meters depending on water clarity (e.g., Lee et al., 2007). Based on our observations at mooring sites, the subsurface chlorophyll maxima (SCM; ~25–50 m) appear to be seasonally persistent in the Amundsen Gulf. In fact, we do not know if the surface POC images derived from MODIS correctly accounted for the presence of these features. Moreover, two contrasting hypotheses can explain the development of SCM in the region: (1) they are linked to the usual decline of primary production as nutrients become depleted in the stratified surface layer in late summer (Carmack et al., 2004); or (2) they form early in the season because the lower part of the euphotic zone provides a suitable environment to shade-adapted algae when nutrient supply near the surface is already weak (Tremblay et al., 2008). Here, while we know that the SCM developed as early as June in 2004, we cannot confirm that the SCM detected in September or October 2003, 2005 and 2006 reflected a recurrent structure or were linked to the normal depletion of nutrients in the surface layer. Clearly, more studies are urgently needed to resolve the importance of SCM for carbon fluxes and for the applicability of satellite algorithms in the southeastern Beaufort Sea.

4.4. Relationships between surface POC and vertical export: clues to the pelagic retention?

The coupling between POC production in the surface layer and the flux to deeper waters depends on the sinking rates of particles, mediation by heterotrophic plankton populations and lateral transport in or out of the sampling location (e.g., Smith and Dunbar, 1998; Buesseler et al., 2008). Although our satellite composite images cannot be used to calculate the production rates of POC, the estimated surface POC concentrations provided coherent relationships with the vertical POC fluxes recorded at 100 m depth. These relations were more convincing ($r>0.70$) when using the circles of 5 and 25 km radius than with the 50 km radius area (r=0.53). That vertical POC fluxes were more representative of a geographic zone less than $2000\,km^2$ is in agreement with the modeling study of Siegel et al. (2008), which determined that source funnels of upper-ocean traps (~150 m) are typically less than 25 km radial distance over 5-day collections. In addition, the average slope of the three linear regressions using the 100 m fluxes suggests that ~30% of the surface POC pool is exported to 100 m depth in the ice-free waters of the Amundsen Gulf, when both surface and flux values are integrated over 2-week periods. Our results may be compared with those of Reigstad et al. (2008) for the eastern Arctic (i.e., Barents Sea and Amundsen Basin), which showed that ~36% of the daily primary production from March to July was exported as POC to 90 m depth. Analogous fractions (27–35%) of the primary production exported below the euphotic layer were estimated during the ice-reduced

season in the North Water Polynya (Caron et al., 2004; Tremblay et al., 2006).

On the other hand, our relationships might suggest that POC fluxes at 100 m depth were affected to the same degree by zooplankton control over the years, although this is contradictory to what the cold vs. warm year scenarios implied (see above). Thus, we underscore that when the data from the cold summer of 2006 were removed from the regressions of the 100 m fluxes on surface POC concentrations, the mean slope decreased from ~30% to ~10%. At first glance, this result may strengthen the idea that vertical export during the years of early ice break-up is not well coupled with primary production due to enhanced zooplankton grazing (Bluhm and Gradinger, 2008). However, the correlations without the data from 2006 were not significant ($p > 0.32$). Therefore, we conclude that the multi-year average of POC retention in the upper 100 m of Amundsen Gulf may be roughly estimated to 70%, even if the retention appears to be even greater in the years when phytoplankton production does not develop as an ice edge bloom. An additional explanation for the lack of coupling between surface POC and vertical export at 100 m depth when the 2006 data are removed from the regressions could be the inter-annual variability of water flow above the sediment trap. Strong current velocities were recorded at 80 m depth during the summers of 2004 and 2005 (up to 40 cm s^{-1}), while circulation remained weak (< 12 cm s^{-1}) in 2006. Currents > 12 cm s^{-1} perturb the collection efficiency of sediment traps by decreasing the consistency between settling particles *in situ* and trap-collected particles (Gardner, 1985; Baker et al., 1988). Hence, it is possible that the vertical fluxes measured by the Technicap trap in the summers of 2004 and 2005 were not accurate because tilting of cylindrical traps may produce under- or over-collection. But even if this may partly explain why the 100 m fluxes did not show a relationship with surface POC when the data from 2006 were excluded, we assume that hydrodynamic biases were negligible since the mooring did not tilt more than 4° during these periods—which is an angle that would not affect the trap-collection efficiency (Gardner, 1985).

The absence of any relationship between surface POC and vertical POC fluxes at 210 m depth suggests that strong attenuation and transformation of sinking particles occur in the epipelagic zone of the western Amundsen Gulf. The overall absence of connection between particle fluxes at 100 and 210 m depth is also in agreement with the notion of a 'pelagic mill' (*sensu* Wassmann et al., 2003) that heavily recycles settling POC in the water column. So is the significant increase of C:N ratios between these two depths, illustrating that sinking biogenic particles were more and more processed with depth (e.g., Lalande et al., 2007). Conversely, the slopes (0.20 and 0.40) of the significant correlations ($p \leq 0.03$) of POC fluxes at 210 m against the 100 m values – if only related for the same periods as the satellite images – enable us to estimate that 4–6% (i.e., 20–40% of 30–10%) of the surface POC reservoir actually reached the inferior limit of the Pacific Halocline in open water (see Section 3.5). Except for an episodic increase of up to 20 cm s^{-1} in early July 2005, current speeds at ~200 m remained low (< 12 cm s^{-1}) during the successive ice-free periods of 2004, 2005 and 2006. Hence, the 210 m sediment trap is assumed to be exempt of any strong bias related to current velocities. However, the problem of collection efficiency depends not only on trap hydrodynamics, but also on the characteristics of settling particles. Conical traps tend to under-collect carbon-rich particles which can be swept in and out by the flow circulating into the trap, even if such funnel clearance is usually prevented by the use of baffles which reduce turbulence and retain particles in the collector (Buesseler et al., 2007). In our study, POC-rich material obviously settled to depth in summer, and especially in 2006 when an ice edge bloom developed in the western Amundsen Gulf. Thus, while we are confident that the particles collected by the Nichiyu conical trap at 210 m are representative of the actual mass flux *in situ*, we cannot confirm without any doubt that this is true for POC-rich particles. Although not significant (p=0.09), the negative trend (r=−0.22) between sinking POC and current speeds around 200 m depth is an additional sign of suspicion against the conical trap.

Nevertheless, our results of vertical POC flux attenuation are in agreement with Tremblay et al. (2006), who estimated that only ~1% of the primary production reached the benthos over deep sites (~500 m isobath) of the North Water Polynya. That some Arctic ecosystems may not be characterized by relatively high export ratios and a strong pelagic–benthic coupling is an emerging view that contrasts with other studies (e.g., Reigstad et al., 2008; Tamelander et al., 2008). Clearly, more comparable studies are required to understand the variability of vertical attenuation of POC-rich particle fluxes and to identify the key players of pelagic POC retention in pan-Arctic seas.

5. Conclusions

Our assessment of vertical POC fluxes and their environmental co-variables in the western Amundsen Gulf over the years 2004–2006 revealed three distinct scenarios between sea ice conditions, surface POC concentrations and vertical POC export at 100 m: (1) a year of persistent stratification affected by the increasing presence of old sea ice and during which weak primary production as well as low vertical POC fluxes were recorded (2004); (2) a year of early ice break-up and lengthened ice-free period that allowed an extended season of surface POC production near-shore but an intermediate increase of downward POC fluxes offshore (2005); and (3) a year of late ice melt that gave rise to a spring bloom associated to the ice margin and to large vertical POC fluxes also related to supplementary ice-flushed particles (2006). Contrary to our initial hypothesis, the greatest vertical POC export was not recorded during a year of protracted ice-free conditions, but rather in a year when the ice cover retreated late, starting eastward of Cape Parry.

Consequently, the timing of ice cover melt appears crucial in determining the patterns of surface POC production and vertical export in the western Amundsen Gulf. Our observations illustrated that the pulsed ice edge bloom, which is traditionally viewed as a synonym of pelagic–benthic coupling (Bluhm and Gradinger, 2008), occurred only when the fast ice bridge did not form. In the years when sea ice retreated early near Cape Bathurst, elevated surface POC concentrations were topographically linked to the southwestern shallow areas, while weak primary production presumably developed at depth beyond the 200 m isobath (Tremblay et al., 2008). Over the three ice-reduced seasons, the vertical export at 100 m depth corresponded at best to ca. 30% of the surface POC reservoir and was probably even lower in the years of warm surface temperatures. Regardless of the inter-annual variability, the estimated fraction of surface POC concentrations reaching the 210 m water depth was reduced to ~5%. Although we could not resolve the exact physical or biological mechanisms for such a vertical attenuation, our results support that most of settling particles in the Cape Bathurst Polynya are exploited by zooplankton populations and/or redirected toward remineralization (Seuthe et al., 2007; Darnis et al., 2008; Simpson et al., 2008)

Given the recent loss of multi-year ice inputs and the possible decline of the consolidation of the fast ice bridge in the future (David Barber, University of Manitoba, personal communication), upper-ocean POC concentrations in the Amundsen Gulf could potentially increase, since pulsed ice edge blooms – which are not

a common feature in this region (Arrigo and van Dijken, 2004) – seem to be promoted in such conditions. In turn, this could benefit to the pelagic food webs that appear to take advantage of whatever surface POC pool is available during the ice-reduced periods. However, recent analyses suggest that primary production in the Arctic seas depends more on the interplay between nutrient inputs and upper-ocean stratification than on favorable ice and light conditions (Tremblay and Gagnon, 2009). In addition, the degree of match or mismatch between organic carbon production and heterotrophic consumers may be altered depending on shifts in zooplankton life strategies (e.g., Hunt et al., 2008). Hence, a better characterization of the pelagic food web structure and function, along with an improved resolution of primary production and vertical particle fluxes, are needed to elucidate the different pathways of POC flow during the current phase of changing ice conditions in the southeastern Beaufort Sea.

Acknowledgements

We express gratitude to the officers and crew members of the *CCGS Amundsen* for professional and enthusiastic assistance at sea. We acknowledge the CASES/ArcticNet mooring teams: L. Michaud, S. Blondeau, P. Massot, G. Desmeules, G. Ingram, B. van Hardenberg and D. Sieberg. We thank A.C. Bélisle, B. Valdenaire, L. Létourneau, G. Darnis, D. Robert, H. Hattori and R. Makabe for help at sea or in the laboratory. We are highly grateful to P. Larouche and M. Gosselin for sharing their data to produce the regional POC algorithm. We thank T. Poulain for the surface POC extractions. Special thanks to Y. Gratton, M.E. Rail, V. Lago and P. Guillot for the processing of CTD, moored T (°C)-probe and current meter data; and to J.É. Tremblay and J. Martin for the fluorometer calibration factors. We thank the CASES/ArcticNet coordinators M. Fortier, M. Ringuette, J. Michaud and K. Lévesque for the organization of the fieldwork and workshops. We gratefully thank the DSRI associate editor Dr. Tom Trull and three anonymous reviewers for insightful comments that greatly strengthened and improved the initial manuscript. The Research Network CASES is funded by the Natural Sciences and Engineering Research Council of Canada (NSERC) and the Canada Foundation for Innovation. The ArcticNet Network is funded by the program of Networks of Centres of Excellence (NCE) of Canada. AF benefited from scholarships from NSERC, Indian and Northern Affairs Canada, the W. Garfield Weston Foundation and the Fonds québécois de la recherche sur la nature et les technologies. This is a joint contribution to the research programs of Québec-Océan, CASES and ArcticNet, and to the Canada Research Chair on the response of marine Arctic ecosystems to climate warming.

Appendix. Development and validation of the regional POC algorithm

During the Canadian Arctic Shelf Exchange Study in June and July 2004, >50 stations covering the wide spectrum of hydrographical conditions present in the southern Beaufort Sea were sampled to develop and validate empirical algorithms for estimating the contribution of colored dissolved organic matter (CDOM) to total light absorption (see Bélanger et al., 2008, for exact sampling locations) and for estimating POC from remote-sensing reflectance. Water samples were collected from the sea surface using a clean bucket deployed from the front deck of the ship. Triplicate water samples (0.5–2.5 L depending on particulate concentration) were filtrated onto pre-combusted (450 °C, for 6 h) GFF filters (25 mm, 0.7 μm pore-size, Whatman) under low vacuum. The GFF filters were then stored frozen at −80 °C until they were analyzed in the land-based laboratory (Maurice-Lamontagne Institute, Mont-Joli, Canada). Triplicate samples for total particulate carbon (TPC, mg m^{-3}) were determined using a Perkin-Elmer CHN 2400 Elemental Analyzer. Triplicate analyses were averaged for TPC. Coefficient of variation (c.v.) was on averaged 9% for all triplicates. When c.v. was >10%, the outlier was not taken into account for the TPC calculation. POC was not determined directly on these samples. At some stations, however, suspended TPC and POC were determined in the water column. At each of these stations, the POC represented more than 80% of the TPC with average of 91% ± 11% (± standard variation; n=21) for surface pelagic waters (Michel Gosselin, Université du Québec à Rimouski, personal communication), a value identical to the finding of Juul-Pedersen et al. (2008). We therefore calculated the surface POC concentrations assuming that POC was equal to 91% TPC.

Optical measurements for the determination of the spectral remote-sensing reflectance ($R_{rs}(\lambda)$, sr^{-1}) were carried out after the surface water sampling. A detailed description of these measurements can be found in Bélanger et al. (2008) and the methodology in Mueller et al. (2003). The database includes both Case 1 and Case 2 waters with a dominance of stations influenced by a relatively high abundance of CDOM relative to the other optical constituents. Forty-eight R_{rs} spectra were used in the development of the regional POC algorithm.

A small number of satellite-based POC algorithms have recently been developed, demonstrating the potential of ocean color remote-sensing in estimating POC from space (e.g., Stramski et al., 1999; Gardner et al., 2006). Using a dataset obtained in the north polar Atlantic and SeaWiFS imagery, Stramska and Stramski (2005) analyzed different approaches to estimate POC from remote-sensing reflectance. They concluded that an algorithm based on the blue-to-green ratio of R_{rs} provides the most robust way to estimate POC from satellite imagery. Building upon these findings, we developed a regional POC algorithm for the Amundsen Gulf that makes use of the ratio of $R_{rs}(490)/R_{rs}(555)$ (Fig. 11). This ratio was favored over the ratio $R_{rs}(443)/R_{rs}(555)$, also proposed by Stramska and Stramski (2005), because of the higher concentration of CDOM in our study area compared to global oceanic waters, which affects more strongly the reflectance spectrum at this wavelength. The regression equation for the

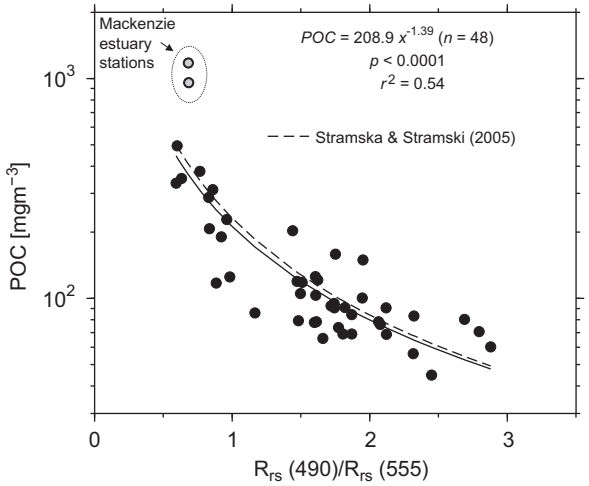

Fig. 11. Relationship between POC and the blue-to-green ratio of remote-sensing reflectance (490, 555 nm) measured during the CASES 2004 field campaign. The dashed line shows the relationship between POC and the same ratio given by Stramska and Stramski (2005) for the US JGOFS and the NASA Sensor Intercomparison for Marine Biological and Interdisciplinary Ocean Studies (SIMBIOS) programs (their Algorithm 4).

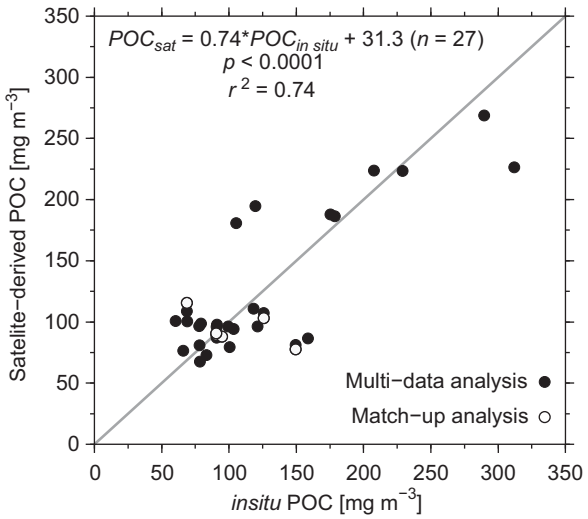

Fig. 12. Comparison of satellite-derived POC and *in situ* data obtained during the CASES 2004 field campaign. The match-up analysis consisted in comparing the remote-sensing data collected within <6 h of the *in situ* sampling time to the *in situ* surface POC concentration, whereas the 2-week average method compared the multi-date POC composites to *in situ* POC data collected during the time interval of the composite (see the Appendix for details).

CASES dataset is

$$\mathrm{POC} = 208.9\left[\frac{R_{rs}(490)}{R_{rs}(555)}\right]^{-1.39}, \quad r^2 = 0.54, \ n = 48. \tag{1}$$

when the two stations located in the Mackenzie estuary are excluded from the analysis (POC=968.7 and 1132.7 mg C m^{-3}), the r^2 reaches 0.81.

A comparison of satellite-derived POC and *in situ* data was performed using the data obtained during the CASES 2004 field campaign. Here, two different approaches were adopted to validate the satellite data product. The first one consisted in comparing the remote-sensing data collected within <6 h of the *in situ* sampling time (referred to as a match-up analysis) to the *in situ* POC concentration. Strictly speaking, a validation of satellite products should always be made with a match-up analysis, but only six match-ups were available for the study area. An alternative method, which consisted in comparing the multi-date POC composites to *in situ* POC data collected during the time interval of the composite (referred to as a multi-date analysis), was also explored to enhance the reliability of the satellite data. The results of the match-up and the multi-date analysis are shown in Fig. 12. The mean normalized bias and the normalized root mean square error for the match-up analysis (n=6) are -1.2% and 38.2%, respectively, and -1.3% and 17.7% for the multi-date analysis (n=27), respectively. The later numbers are in the same order as the POC algorithms performance reported by Stramska and Stramski (2005) despite the fact that our multi-date analysis may be affected by a gap between the satellite and *in situ* sampling time. These results suggest that MODIS perform well in the estimation of POC in the study area. The blue-to-green ratio of R_{rs} is correlated to the particulate beam attenuation at 660 nm (a good proxy for POC) and this relationship is not affected by the seasonal variability in the phytoplankton optical properties (Gardner et al., 2006; Stramska et al., 2006). Interestingly, our empirical POC algorithm is consistent with the algorithms based on the blue-to-green ratio of R_{rs} published by Stramska and Stramski (2005), which suggests that the POC-specific inherent optical properties found in the southeastern Beaufort Sea may be similar to waters found elsewhere in the ocean.

It should be mentioned that a POC algorithm based on particulate backscattering coefficient at 555 nm ($b_{bp}(555)$), as derived using a quasi-analytical algorithm (Lee et al., 2002), performed better than the blue-to-green ratio-based algorithm (r^2=0.89) when applied to *in situ* data. However, when applied to satellite data, the $b_{bp}(555)$-based algorithm introduced noise (r^2=0.26 for a linear regression between $\mathrm{POC_{sat}}$ and $\mathrm{POC_{in\ situ}}$), especially near sea ice. This noise is very likely due to an adjacency effect or sub-pixel contamination by sea ice (see Bélanger et al., 2007).

References

Amiel, D., Cochran, J.K., 2008. Terrestrial and marine POC fluxes derived from ^{234}Th distributions and δ^{13}C measurements on the Mackenzie River Shelf. J. Geophys. Res. 113, C03S06.

Arrigo, K.R., van Dijken, G.L., 2004. Annual cycles of sea ice and phytoplankton in Cape Bathurst polynya, southeastern Beaufort Sea, Canadian Arctic. Geophys. Res. Lett. 31, L08304.

Arrigo, K.R., van Dijken, G., Pabi, S., 2008. Impact of a shrinking Arctic ice cover on marine primary production. Geophys. Res. Lett. 35, L19603.

Ayles, G.B., Snow, N.B., 2002. Canadian Beaufort Sea 2000: the environmental and social setting. Arctic 55, 4–17.

Backhaus, J.O., Fohrmann, H., Kaempf, J., Rubino, A., 1997. Formation and export of water masses produced in Arctic shelf polynyas—process studies of oceanic convection. ICES J. Mar. Sci. 54 (3), 366–382.

Baker, E.T., Milburn, H.B., Tennant, D.A., 1988. Field assessment of sediment trap efficiency under varying flow conditions. J. Mar. Res. 46 (13), 573–592.

Banse, K., English, D.C., 1999. Comparing phytoplankton seasonality in the eastern and western subarctic Pacific and the western Bering Sea. Prog. Oceanogr. 43 (2–4), 235–287.

Bates, N.R., Moran, S.B., Hansell, D.A., Mathis, J.T., 2006. An increasing CO_2 sink in the Arctic Ocean due to sea-ice loss. Geophys. Res. Lett. 33, L23609.

Bélanger, S., Ehn, J.K., Babin, M., 2007. Impact of sea ice on the retrieval of water-leaving reflectance, chlorophyll a concentration and inherent optical properties from satellite ocean color data. Remote Sensing Environ. 111 (1), 51–68.

Bélanger, S., Babin, M., Larouche, P., 2008. An empirical ocean color algorithm for estimating the contribution of chromophoric dissolved organic matter to total light absorption in optically complex waters. J. Geophys. Res. 113, C04027.

Bessière, A., Nozais, C., Brugel, S., Demers, S., Desrosiers, G., 2007. Metazoan meiofauna dynamics and pelagic–benthic coupling in the Southeastern Beaufort Sea, Arctic Ocean. Polar Biol. 30 (9), 1123–1135.

Bluhm, B.A., Gradinger, R., 2008. Regional variability in food availability for Arctic marine mammals. Ecol. Appl. 18 (sp2), S77–S96.

Boyd, P.W., Trull, T.W., 2007. Understanding the export of biogenic particles in oceanic waters: is there consensus? Prog. Oceanogr. 72 (4), 276–312.

Brugel, S., Nozais, C., Poulin, M., Tremblay, J.E., Miller, L.A., Simpson, K.G., Gratton, Y., Demers, S., 2009. Phytoplankton biomass and production in the southeastern Beaufort Sea in autumn 2002 and 2003. Mar. Ecol. Prog. Ser. 377, 63–77.

Buesseler, K.O., Antia, A.N., Chen, M., Fowler, S.W., Gardner, W.D., Gustafsson, O., Harada, K., Michaels, A.F., van der Loeff, M., Sarin, M., 2007. An assessment of the use of sediment traps for estimating upper ocean particle fluxes. J. Mar. Res. 65 (3), 345–416.

Buesseler, K.O., Trull, T.W., Steinberg, D.K., Silver, M.W., Siegel, D.A., Saitoh, S.I., Lamborg, C.H., Lam, P.J., Karl, D.M., Jiao, N.Z., Honda, M.C., Elskens, M., Dehairs, F., Brown, S.L., Boyd, P.W., Bishop, J.K.B., Bidigare, R.R., 2008. VERTIGO (VERtical transport in the global ocean): a study of particle sources and flux attenuation in the North Pacific. Deep-Sea Res. II 55 (14–15), 1522–1539.

Carmack, E., Barber, D., Christensen, J., Macdonald, R., Rudels, B., Sakshaug, E., 2006. Climate variability and physical forcing of the food webs and the carbon budget on panarctic shelves. Prog. Oceanogr. 71 (2–4), 145–181.

Carmack, E., Chapman, D.C., 2003. Wind-driven shelf/basin exchange on an Arctic shelf: the joint roles of ice cover extent and shelf-break bathymetry. Geophys. Res. Lett. 30 (14), 1778.

Carmack, E.C., MacDonald, R.W., 2002. Oceanography of the Canadian Shelf of the Beaufort Sea: a setting for marine life. Arctic 55 (Suppl. 1), 29–45.

Carmack, E.C., Macdonald, R.W., Jasper, S., 2004. Phytoplankton productivity on the Canadian Shelf of the Beaufort Sea. Mar. Ecol. Prog. Ser. 277, 37–50.

Caron, G., Michel, C., Gosselin, M., 2004. Seasonal contributions of phytoplankton and fecal pellets to the organic carbon sinking flux in the North Water (northern Baffin Bay). Mar. Ecol. Prog. Ser. 283, 1–13.

CIS, 2007. Amundsen Gulf Animation 1980–2007. 〈http://ice-glaces.ec.gc.ca/content_contenu/anim/amundsen_animation.gif〉.

Conlan, K., Aitken, A., Hendrycks, E., McClelland, C., Melling, H., 2008. Distribution patterns of Canadian Beaufort Shelf macrobenthos. J. Mar. Sys. 74 (3–4), 864–886.

Crease, J., 1988. The acquisition, calibration and analysis of CTD data. Unesco Technical Papers in Marine Science No. 54. (A Report of SCOR Working Group 51), Division of Marine Sciences, UNESCO, Paris, France.

Darnis, G., Barber, D.G., Fortier, L., 2008. Sea ice and the onshore-offshore gradient in pre-winter zooplankton assemblages in south-eastern Beaufort Sea. J. Mar. Sys. 74 (3–4), 994–1011.

Emmerton, C.A., Lesack, L.F.W., Vincent, W.F., 2008. Nutrient and organic matter patterns across the Mackenzie River, estuary and shelf during the seasonal recession of sea-ice. J. Mar. Sys. 74 (3–4), 741–755.

Engel, A., Passow, U., 2001. Carbon and nitrogen content of transparent exopolymer particles (TEP) in relation to their Alcian Blue adsorption. Mar. Ecol. Prog. Ser. 219, 1–10.

Fischer, G., Donner, B., Ratmeyer, V., Davenport, R., Wefer, G., 1996. Distinct year-to-year particle flux variations off Cape Blanc during 1988–1991: relation to delta18O-deduced sea-surface temperatures and trade winds. J. Mar. Res. 54 (1), 73–98.

Forest, A., Sampei, M., Hattori, H., Makabe, R., Sasaki, H., Fukuchi, M., Wassmann, P., Fortier, L., 2007. Particulate organic carbon fluxes on the slope of the Mackenzie Shelf (Beaufort Sea): physical and biological forcing of shelf-basin exchanges. J. Mar. Sys. 68, 39–54.

Forest, A., Sampei, M., Makabe, R., Sasaki, H., Barber, D., Gratton, Y., Wassmann, P., Fortier, L., 2008a. The annual cycle of particulate organic carbon export in Franklin Bay (Canadian Arctic): environmental control and food web implications. J. Geophys. Res. 113, C03S05.

Forest, A., Sampei, M., Rail, M.E., Gratton, Y., Fortier, L., 2008b. Winter pulses of Pacific-origin water and resuspension events along the Canadian Beaufort Slope revealed by a bottom-moored observatory. In: Proceedings of MTS/IEEE Oceans 2008: Oceans, Poles, and Climate—Technological Challenges, Québec, Canada, 15–18 September 2008. doi:10.1109/OCEANS.2008.5152010.

Franz, B.A., 2005. Msl12 User's Guide. 〈http://oceancolor.gsfc.nasa.gov/DOCS/MSL12/〉.

Galley, R.J., Key, E., Barber, D.G., Hwang, B.J., Ehn, J.K., 2008. Spatial and temporal variability of sea ice in the southern Beaufort Sea and Amundsen Gulf: 1980–2004. J. Geophys. Res. 113, C05S95.

Gardner, W.D., 1985. The effect of tilt on sediment trap efficiency. Deep-Sea Res. A32 (3A), 349–361.

Gardner, W.D., Mishonov, A.V., Richardson, M.J., 2006. Global POC concentrations from in-situ and satellite data. Deep-Sea Res. II 53 (5–7), 718–740.

Garneau, M.E., Roy, S., Pedrós-Alió, C., Lovejoy, C., Gratton, Y., Vincent, W.F., 2008. Seasonal dynamics of bacterial biomass and production in a coastal arctic ecosystem: Franklin Bay, western Canadian Arctic. J. Geophys. Res. 113, C07S91.

Hargrave, B.T., Walsh, I.D., Murray, D.W., 2002. Seasonal and spatial patterns in mass and organic matter sedimentation in the North Water. Deep-Sea Res. II 49 (22–23), 5227–5244.

Honjo, S., Manganini, S.J., Krishfield, R.A., Francois, R., 2008. Particulate organic carbon fluxes to the ocean interior and factors controlling the biological pump: a synthesis of global sediment trap programs since 1983. Prog. Oceanogr. 76 (3), 217–285.

Hunt Jr., G.L., Stabeno, P.J., Strom, S., Napp, J.M., 2008. Patterns of spatial and temporal variation in the marine ecosystem of the southeastern Bering Sea, with special reference to the Pribilof Domain. Deep-Sea Res. Part II 55 (16–17), 1919–1944.

Hwang, J., Eglinton, T.I., Krishfield, R.A., Manganini, S.J., Honjo, S., 2008. Lateral organic carbon supply to the deep Canada Basin. Geophys. Res. Lett. 35, L11607.

Ingram, R.G., Williams, W.J., van Hardenberg, B., Dawe, J.T., Carmack, E., 2008. Seasonal circulation over the Canadian Beaufort Shelf. In: Fortier, L., Barber, D.G., Michaud, J. (Eds.), On Thin Ice: A Synthesis of the Canadian Arctic Shelf Exchange Study (CASES). Aboriginal Issues Press, Winnipeg, pp. 13–38.

Jin, M., Deal, C., Wang, J., Alexander, V., Gradinger, R., Saitoh, S., Iida, T., Wan, Z., Stabeno, P., 2007. Ice-associated phytoplankton blooms in the southeastern Bering Sea. Geophys. Res. Lett. 34, L06612.

Juul-Pedersen, T., Michel, C., Gosselin, M., Seuthe, L., 2008. Seasonal changes in the sinking export of particulate material under first-year sea ice on the Mackenzie Shelf (western Canadian Arctic). Mar. Ecol. Prog. Ser. 353, 13–25.

Knap, A., Michaels, A., Close, A., Ducklow, H., Dickson, A., 1996. Protocols for the Joint Global Ocean Flux Study (JGOFS) Core Measurements. JGOFS Report Nr 19, pp. 155–162.

Kowalik, Z., Proshutinsky, A.Y., 1994. The Arctic Ocean tides. In: Johannessen, O.M., Muench, R.D., Overland, J.E. (Eds.), The Polar Oceans and Their Role in Shaping the Global Environment. American Geophysical Union, USA, pp. 137–158.

Lalande, C., Grebmeier, J.M., Wassmann, P., Cooper, L.W., Flint, M.V., Sergeeva, V.M., 2007. Export fluxes of biogenic matter in the presence and absence of seasonal sea ice cover in the Chukchi Sea. Cont. Shelf Res. 27 (15), 2051–2065.

Lee, Z., Carder, K.L., Arnone, R.A., 2002. Deriving inherent optical properties from water color: a multiband quasi-analytical algorithm for optically deep waters. Appl. Opt. 41 (27), 5755–5772.

Lee, I.H., Liu, J.T., 2006. Rectification of the heading and tilting of sediment trap arrays due to strong tidal currents in a submarine canyon. Geophys. Res. Lett. 33, L08609.

Lee, Z., Weidemann, A., Kindle, J., Arnone, R., Carder, K.L., Davis, C., 2007. Euphotic zone depth: its derivation and implication to ocean-color remote sensing. J. Geophys. Res. 112, C03009.

Lepore, K., Moran, S.B., Grebmeier, J.M., Cooper, L.W., Lalande, C., Maslowski, W., Hill, V., Bates, N.R., Hansell, D.A., Mathis, J.T., 2007. Seasonal and interannual changes in particulate organic carbon export and deposition in the Chukchi Sea. J. Geophys. Res. 112 (10), C10024.

Loeng, H., Brander, K., Carmack, E., Denisenko, S., Drinkwater, K., Hansen, B., Kovacs, K., Livingston, P., 2005. Marine systems. In: Symon, C., Arris, L., Heal, B. (Eds.), Arctic Climate Impact Assessment. Cambridge University Press, New York, pp. 454–522.

Lukovich, J.V., Barber, D.G., 2006. Atmospheric controls on sea ice motion in the southern Beaufort Sea. J. Geophys. Res. 111, D18103.

Meiners, K., Gradinger, R., Gehling, J., Civitarese, G., Spindler, M., 2003. Vertical distribution of exopolymer particles in sea ice of the Fram Strait (Arctic) during autumn. Mar. Ecol. Prog. Ser. 248, 1–13.

Michel, C., Ingram, R.G., Harris, L.R., 2006. Variability in oceanographic and ecological processes in the Canadian Arctic Archipelago. Prog. Oceanogr. 71 (2–4), 379–401.

Morata, N., Renaud, P.E., Brugel, S., Hobson, K.A., Johnson, B.J., 2008. Spatial and seasonal variations in the pelagic–benthic coupling of the southeastern Beaufort Sea revealed by sedimentary biomarkers. Mar. Ecol. Prog. Ser. 371, 47–63.

Mucci, A., Forest, A., Fortier, L., Fukuchi, M., Grant, J., Hattori, H., Hill, P., Lintern, G., Makabe, R., Magen, C., Miller, L., Sampei, M., Sasaki, H., Sundby, B., Walker, T., Wassmann, P., 2008. Organic and inorganic fluxes. In: Fortier, L., Barber, D.G., Michaud, J. (Eds.), On Thin Ice: A Synthesis of the Canadian Arctic Shelf Exchange Study (CASES). Aboriginal Issues Press, Winnipeg, pp. 117–146.

Mueller, J.L., Morel, A., Frouin, R., Davis, C., Arnone, R.A., Carder, K.L., Lee, Z.-P., Stewart, R.G., Hooker, S.B., Holben, B., Mobley, C.D., McLean, S., Miller, M., Pietras, C., Fargion, G.S., Knobelspiesse, K.D., Voss, K., 2003. Radiometric measurements and data analysis protocols. In: Mueller, J.L., Fargion, G.S., McClain, C.R. (Eds.), Ocean Optics Protocols for Satellite Ocean Color Sensor Validation, vol. III. NASA Goddard Space Flight Center, Greenbelt, pp. 1–78 (revision 4).

NCDC, 2009. National Climatic Data Center. Climate Monitoring: State of the Climate, National Oceanic and Atmospheric Administration, Global Surface Temperature Anomalies 〈ftp://ftp.ncdc.noaa.gov/pub/data/anomalies/annual.land_and_ocean.90S.90N.df_1901-2000mean.dat〉.

Nodder, S.D., Boyd, P.W., Chiswell, S.M., Pinkerton, M.H., Bradford-Grieve, J.M., Greig, M.J.N., 2005. Temporal coupling between surface and deep ocean biogeochemical processes in contrasting subtropical and subantarctic water masses, southwest Pacific Ocean. J. Geophys. Res. 110, C12017.

O'Brien, M.C., Macdonald, R.W., Melling, H., Iseki, K., 2006. Particle fluxes and geochemistry on the Canadian Beaufort Shelf: implications for sediment transport and deposition. Cont. Shelf Res. 26 (1), 41–81.

Pabi, S., van Dijken, G.L., Arrigo, K.R., 2008. Primary production in the Arctic Ocean, 1998–2006. J. Geophys. Res. 113, C08005.

Rachold, V., Eicken, H., Gordeev, V.V., Grigoriev, M.N., Hubberten, H.W., Lisitzin, A.P., Shevchenko, V.P., Schirrmeister, L., 2004. Modern terrigenous organic carbon input to the Arctic Ocean. In: Stein, R., MacDonald, R.W. (Eds.), The Organic Carbon Cycle in the Arctic Ocean. Springer-Verlag, New York, pp. 33–54.

Ramseier, R.O., Garrity, C., Bauerfeind, E., Peinert, R., 1999. Sea-ice impact on long-term particle flux in the Greenland Sea's Is Odden-Nordbukta region, 1985–1996. J. Geophys. Res. 104 (C3), 5329–5343.

Reigstad, M., Wexels Riser, C., Wassmann, P., Ratkova, T., 2008. Vertical export of particulate organic carbon: attenuation, composition and loss rates in the northern Barents Sea. Deep-Sea Res. II 55 (20–21), 2308–2319.

Renaud, P.E., Riedel, A., Michel, C., Morata, N., Gosselin, M., Juul-Pedersen, T., Chiuchiolo, A., 2007. Seasonal variation in benthic community oxygen demand: a response to an ice algal bloom in the Beaufort Sea, Canadian Arctic? J. Mar. Sys. 67 (1–2), 1–12.

Riedel, A., Michel, C., Gosselin, M., 2006. Seasonal study of sea-ice exopolymeric substances on the Mackenzie shelf: implications for transport of sea-ice bacteria and algae. Aquat. Microb. Ecol. 45, 195–206.

Sakshaug, E., 2004. Primary and secondary production in the Arctic Seas. In: Stein, R., MacDonald, R.W. (Eds.), The Organic Carbon Cycle in the Arctic Ocean. Springer-Verlag, New York, pp. 57–81.

Sampei, M., Sasaki, H., Hattori, H., Fukuchi, M., Hargrave, B.T., 2004. Fate of sinking particles, especially fecal pellets, within the epipelagic zone in the North Water (NOW) polynya of northern Baffin Bay. Mar. Ecol. Prog. Ser. 278, 17–25.

Sasaki, H., Forest, A., Sampei, M., Makabe, R., Hattori, H., Fukuchi, M., Fortier, L., 2006. Regional variability of downward particle flux in waters of the Mackenzie Shelf slope and the Amundsen Gulf in 2003–2004. In: Proceedings of the CASES 2005–2006 General Meeting Winnipeg, Manitoba, Canada, 13–16 February 2006.

Serreze, M.C., Holland, M.M., Stroeve, J., 2007. Perspectives on the Arctic's Shrinking Sea-Ice Cover. Science 315 (5818), 1533.

Seuthe, L., Darnis, G., Riser, C.W., Wassmann, P., Fortier, L., 2007. Winter–spring feeding and metabolism of Arctic copepods: insights from faecal pellet production and respiration measurements in the southeastern Beaufort Sea. Polar Biol. 30 (4), 427–436.

Siegel, D.A., Fields, E., Buesseler, K.O., 2008. A bottom-up view of the biological pump: modeling source funnels above ocean sediment traps. Deep-Sea Res. I 55 (1), 108–127.

Simpson, K., Tremblay, J.E., Gratton, Y., Price, N.M., 2008. An annual study of inorganic and organic nitrogen and phosphorus, and silicic acid, in the southeastern Beaufort Sea. J. Geophys. Res. 113, C07016.

Smith, J.W.O., Dunbar, R.B., 1998. The relationship between new production and vertical flux on the Ross Sea continental shelf. J. Mar. Sys. 17 (1–4), 445–457.

Stein, R., Macdonald, R.W., 2004. Geochemical proxies used for organic carbon source identification in Arctic Ocean sediments. In: Stein, R., Macdonald, R.W. (Eds.), The Organic Carbon Cycle in the Arctic Ocean. Springer-Verlag, New York, pp. 24–32.

Stramska, M., Stramski, D., 2005. Variability of particulate organic carbon concentration in the north polar Atlantic based on ocean color observations

with Sea-viewing Wide Field-of-view Sensor (SeaWiFs). J. Geophys. Res. 110 (C10), 10018.
Stramska, M., Stramski, D., Kaczmarek, S., Allison, D.B., Schwarz, J., 2006. Seasonal and regional differentiation of bio-optical properties within the north polar Atlantic. J. Geophys. Res. 111, C08003.
Stramski, D., Reynolds, R.A., Kahru, M., Mitchell, B.G., 1999. Estimation of particulate organic carbon in the ocean from satellite remote sensing. Science 285 (5425), 239–242.
Tamelander, T., Reigstad, M., Hop, H., Carroll, M.L., Wassmann, P., 2008. Pelagic and sympagic contribution of organic matter to zooplankton and vertical export in the Barents Sea marginal ice zone. Deep-Sea Res. II 55 (20–21), 2330–2339.
Tremblay, J.-E., Hattori, H., Michel, C., Ringuette, M., Mei, Z.-P., Lovejoy, C., Fortier, L., Hobson, K.A., Amiel, D., Cochran, K., 2006. Trophic structure and pathways of biogenic carbon flow in the eastern North Water Polynya. Prog. Oceanogr. 71 (2–4), 402–425.
Tremblay, J.E., Simpson, K., Martin, J., Miller, L.A., Gratton, Y., Price, N.M., 2008. Vertical stability and the annual dynamics of nutrients and chlorophyll fluorescence in the coastal, southeast Beaufort Sea. J. Geophys. Res. 113, C07S90.
Tremblay, J.E., Gagnon, J., 2009. The effects of irradiance and nutrient supply on the productivity of Arctic waters: a perspective on climate change. In: Nihoul, J.C.J., Kostianoy, A.G. (Eds.), Influence of Climate Change on the Changing Arctic and Sub-Arctic Conditions. Proceedings of the NATO Advanced Research Workshop, Liège, Belgium, 8–10 May 2008. Springer-Verlag, Dordrecht, Netherlands, pp. 73–94.
Turner, J.T., 2002. Zooplankton fecal pellets, marine snow and sinking phytoplankton blooms. Aquat. Microb. Ecol. 27 (1), 57–102.
Venables, H.J., Pollard, R.T., Popova, E.E., 2007. Physical conditions controlling the development of a regular phytoplankton bloom north of the Crozet Plateau, Southern Ocean. Deep-Sea Res. II 54 (18–20), 1949–1965.
Wang, M., Overland, J.E., 2009. A sea ice free summer Arctic within 30 years? Geophys. Res. Lett. 36, L07502.
Wassmann, P., Olli, K., Wexels Riser, C., Svensen, C., 2003. Ecosystem function, biodiversity and vertical flux regulation in the twilight zone. In: Wefer, G., Lamy, F., Mantoura, F. (Eds.), Marine Science Frontiers for Europe. Springer-Verlag, Berlin, pp. 279–287.
Wassmann, P., Bauerfeind, E., Fortier, M., Fukuchi, M., Hargrave, B., Honjo, S., Moran, B., Noji, T., Nöthig, E.M., Peinert, R., 2004. Particulate organic carbon flux to the Arctic Ocean sea floor. In: Stein, R., MacDonald, R. (Eds.), The Organic Carbon Cycle in the Arctic Ocean. Springer-Verlag, New York, pp. 101–138.
Wassmann, P., Slagstad, D., Wexels Riser, C., Reigstad, M., 2006. Modelling the ecosystem dynamics of the Barents Sea including the marginal ice zone: II. Carbon flux and interannual variability. J. Mar. Sys. 59 (1–2), 1–24.